Journal of Proteomics & Bioinformatics

Research Article **Open Access**

Differential Proteomics of the Cerebral Cortex of Juvenile, Adult and Aged Rats: An Ontogenetic Study

Michael Wille[1], Antje Schümann, Michael Kreutzer[2], Michael O Glocker[2], Andreas Wree[1], Grit Mutzbauer[3] and Oliver Schmitt[1*]

[1]Department of Anatomy, Gertrudenstraße 9, 18055 Rostock, Germany
[2]Proteome Center Rostock, Schillingallee 69, 18055 Rostock, Germany
[3]Department of Pathology, Josef-Schneider-Straße 2, 97080 Würzburg, Germany

Abstract

The identification of up- and downregulated as well as absent proteins in the central nervous system is necessary to understand the interplay of migration, differentiation and integration of neuronal progenitor cells at different stages of development. In a first step, differentially expressed proteins of the cerebral cortex of the laboratory rat at three significant stages of development were identified. The cerebral cortex needs differential abundances of proteins during ontogenesis and uses its high plasticity postnatally to adapt to many types of intrinsic and extrinsic changes. This study focuses on the identification of specific proteins which are differentially expressed during postnatal development. Cerebral cortices of P7, P90 and P637 old wistar rats were dissected and analyzed by two-dimensional polyacrylamide gel electrophoresis (2DE) and matrix-assisted laser desorption/ionization time-of-flight mass spectrometry (MALDI-TOF-MS) analysis. The identified and differentially expressed proteins are subdivided into 13 different classes. Proteins of the functional classes of the carbohydrate metabolism, structural and regulatory proteins as well as proteins involved in the energy metabolism show the highest differential abundance within the analyzed stages of development. Cytoskeleton proteins like neurofilaments and β-actin are downregulated in early development. In contrast, some proteins which are necessary for migration and motility are upregulated in P7 versus P90 animals. Furthermore, proteins for vesicular trafficking like drebrin and Gdi2 are upregulated in P7. In aged animals oxidative stress sensors, proteins necessary for autophagy of dysfunctional mitochondria, growth control and hypoxia tolerance (Ppp1ca, Eno1) turned out to be upregulated. Overall, energy consumption and differentiation processes as well as specific regulatory mechanisms can be observed at least indirectly by differential abundances of proteins during the investigated stages of ageing.

Keywords: Brain; Development; Cerebral Cortex; Proteomics; Rat

Abbreviations: A: Axon; CBB: Coomassie Blue; CpG: Cytoplasmic Granule; CNS: Central Nervous System; Cts: Centrosome; Cr: Chromosome; CSK: Cytoskeleton; CP: Chaperones; CPM: Cytoplasm; CPV: Cytoplasmic Vesicle; CTS: Cytosol; Cx: Cerebral Cortex; ECM: Extracellular Matrix; ER: Endoplasmic Reticulum; Eds: Endosome; ExR: Extracellular Region; GC: Growth Cone; GJ: Gap Junction; Golgi: Golgi Apparatus; HGC: Heterotrimeric G-protein Complex; LA: Lipid Anchor; Lyso: Lysosome; M: Membrane; Micro: Microsome; MMT: Mitochondrial Matrix; MM: Mitochondrial Membrane; MIM: Mitochondrion Inner Membrane; MIMS: Mitochondrion Intermembrane Space; MOM: Mitochondrion Outer Membrane; MEL: Melanosome; Mito: Mitochondrion; MT: Microtubule; NC: Nucleus; NF: Neurofilament; NM: Nucleus matrix; NP: Nucleoplasm; P: Proteasome; PA: Proteins Antioxidants; PAAM: Proteins Amino Acid Metabolism; PB: Proteins Biosynthesis; PCM: Proteins Carbohydrate Metabolism; PD: Proteins Degradation; Per: Peroxisome; PEM: Proteins Energy Metabolism; PEMA: Proteinaceous Extracellular Matrix; PFM: Proteins Fat Metabolism; PMP: Peripheral Membrane Protein; PR: Proteins Regulation; PST: Proteins Signal Transduction; PTM: Proteins Transmitter Metabolism; RS: Ribosome; S: Synapse; Sc: Secreted; SCc: Spliceosomal Complex; SER: Smooth Endoplasmic Reticulum; SP: Structural Proteins; SV: Synaptic Vesicle; Ss: Synaptosome; SR: Sarcoplasmic Reticulum; TP: Transport Proteins; ULC: Ubiquitin Ligase Complex

Introduction

Within the intrauterine development from embryonal days (E1-E22) the neurulation occurs during E7 [1,2]. The CNS develops mainly between E14 and E22 [3]. Neuroplasticity is a fundamental process for brain development and neuro-ontogenesis [4]. It describes the property of synapses, neurons and whole brain regions to adapt their properties depending on their biological task. Different types of neuroplasticity are: evolutionary, reactive, adaptive and reparative plasticity [5]. Synaptic plasticity is the most common form of neuroplasticity during aging and it describes the activity-dependent change of the synaptic transmission strength [6]. In addition, cortical plasticity follows the activity-dependent change of the brain size, the connectivity or the activation patterns of cortical networks [7]. Strength and length of stimuli lead to specific interactions of parts of the nervous system which may change the structure of neuronal tissue at the ultrastructural and microscopic level. In terms of differences in the weight of rat brains as well as body mass, changes of the abundance pattern of proteins can be determined. Especially in the first two postnatal months a strong increase in the rats' brain mass occurs. Between postnatal day P2 and P25, the biggest mass increase can be determined, whereas a further increase happens around P60 [8]. Also until P275 an additional mass increase occurs, but on the whole in a decreased and slower pattern [9].

In the first postnatal weeks a considerable number of migratory

processes (e.g. of the glial progenitor cells) are necessary for the development of the CNS. This neuronal migration stops at the time of birth; however, exceptions for different types of cells occur. For example, the migration of neuroblasts in the rostal migratory stream (Figure 1) from the subventricular zone to the olfactory bulb is a physiological process in the adult rat. In addition, neuronal progenitors at the border of the granular cell layer and the hilus show neurogenesis and migrate into the granular layer [10]. The synaptogenesis proceeds in two different phases: early stage (P1-P5) and later stage (P15-P20) [11]. As regards the number of neural and non-neural cells, differences during the development have been observed. While the number of non-neural cells is limited to 4 million cells (ca. 6% of the total cell number) after birth, the number increases up to 140 million cells in the adult rat brain (ca. 50% of the total cell number). A large portion of these non-neural cells originate from the cerebellum (90%). On the whole, the growth of the non-neural cells (except for the cerebellum) is finished by the end of the third postnatal week [8].

The Cx develops from the prosencephalon (Figure 1) [12]. The development of the Cx is subdivided into different phases. Originating from a three-layer structure, the ventricular, the intermediary and the early marginal zone (preplate) build a new layer (cortical layer), located between preplate and intermediary zone. From here the migration of postmitotic neurons (cortical plate) begins where densely packed and radiating arranged cell extensions are visible. The ventricular zone can be divided into an inner and an outer zone. The inner zone shows a higher cell density than the outer zone [13-16]. An immigration of neurons occurs at the base of the cortical plate [17-18]. Differentiation and synaptogenesis are associative, partly overlapping processes [19]. Within the cortical plate, neuronal cell layering can be divided into the upper marginal zone and the underlying subplate [20]. The cells of the subplate show the characteristics of differentiated neurons and, therefore, can process synaptic information from afferent nerve fibers [21]. Additionally, a projection of the neurons themselves into the cortical plate, the thalamus and the colliculus superior is observed [22].

The Cx shows the largest increase of mass during the first postnatal week. In the following weeks of the first postnatal month, the brain
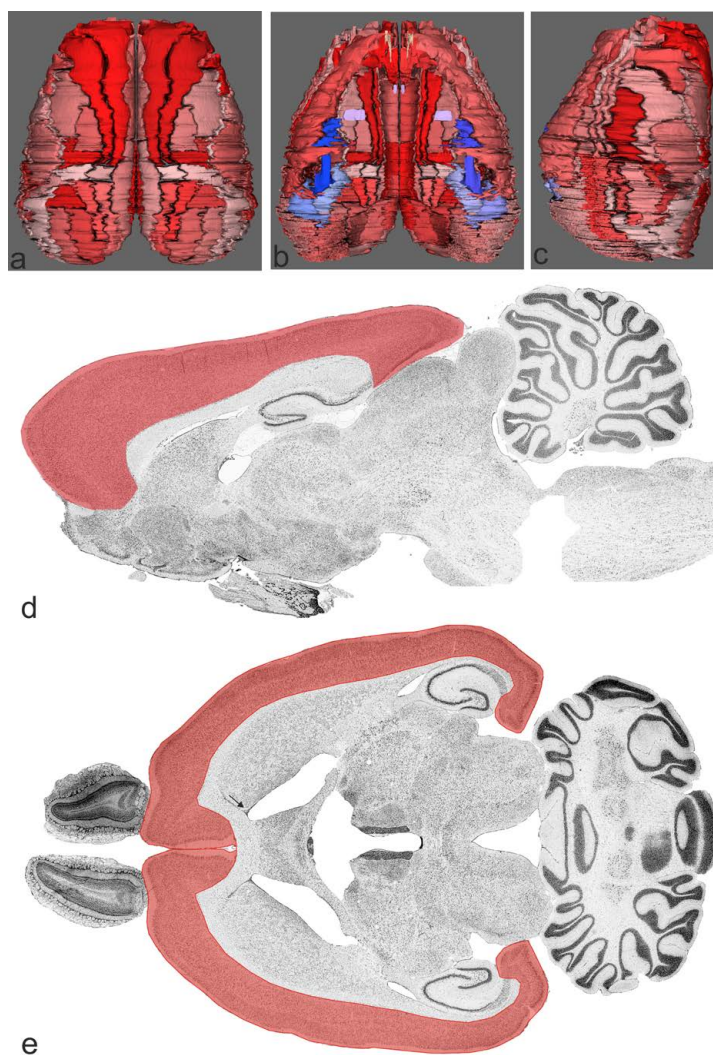
Figure 1: Overview of the rat brain at the level of the Cx. In (a-c) three-dimensional reconstructions of the rat brain from dorsal (a), ventral (b) and lateral (c) are shown. Reconstruction has been build using the neuroVIISAS framework (http://neuroviisas.med.uni-rostock.de/neuroviisas.shtml). (d) A sagittal section with circumscribed cerebral cortex. (e) Horizontal section of the rat cerebral cortex of the left and right hemisphere. The black arrow indicates the source at the rostro-lateral origin of the rostral migratory stream.

grows progressively, although the increase of its mass decelerates. Between P25 and P60, the mass of the brain decreases again, indicating adolescence [8,23]. The remaining increase of neurons in the Cx is relatively small. The largest increase of neurons in the neocortex and the hippocampus takes place within the first days after birth. This initial cortical process of growth leads to the generation of 1-5 million neurons during the first four days after birth. All in all, an increase of about 24 million neurons in the neocortex and about 4 million neurons in the hippocampus is known. After this surplus of neurons in the neocortex and hippocampus, a substantial decrease of the total cell number (60-70% of the neurons within the second postnatal week) occurs.

The aim of this study was to determine the differences in protein abundance during the development and aging of the Cx at ages of the brain P7, P90 and aged individuals at P637. Several studies [24-26] focus on the transplantation of immortalized progenitor cells in 6-OHDA Hemiparkinson animal models [24,25] and the differences in the abundance of this area of the brain at different points of development [26]. Hovakimyan et al. [24] and Haas et al. [25] as well as Schwarz and Freed [27] showed that the micro-environment of neonatal brains seems to be important for the differentiation of transplanted neuronal progenitors. Therefore, a further characterization of the abundance patterns of proteins during development in the Cx of the rat brain might provide a better understanding of neuronal development. The determination of candidate proteins which may support the survival and differentiation of transplanted progenitor cells in neonatal and adult caudate-putamen could serve as targets to optimize transplantation. In the past, different studies were performed which concentrated on the properties of the analyzed cells, but these are not associated with the changes in the CNS. For example, factors like the cell-cell interaction, processes in the signal transduction as well as regulatory processes play an important role. Furthermore, such factors and processes seem to be relevant in influencing the differentiation of neuronal stem cells. Here, we searched for differentially expressed proteins which could be of importance for the neuronal differentiation and for the integration of neuronal progenitors in an adult neuronal environment.

Material and Methods

Treatment

Male Wistar rats (Rattus norvegicus, Charles River, Sulzfeld, Germany) of different ages (7, 90, 637 postnatal days) with n=6 animals in each age group (2 animals per cage) were used for this study [28,29]. The animals were housed at $22 \pm 2°$ C under an artificial day and night rhythm with a 12 h light-dark cycle with free access to water and standard nutrition. The animal treatment and experimental procedures were conducted in compliance with the regulations and licensing of the local authorities (Landesamt für Landwirtschaft, Lebensmittelsicherheit and Fischerei Mecklenburg Vorpommern, Germany) and the Animal Care and Use Committee of the University of Rostock. Pursuant to the European Communities Council Directive of 24 November 1986 (86/609/EEC) and in accordance with the above-mentioned local authorities adequate measures were taken to minimize pain or discomfort.

Perfusion and dissection

At defined dates (7, 90, 637 days postnatal), perfusion was performed. The animals were anesthesized with ether and killed by intraperitoneal Pentobarbital-Na$^+$-injection (60 mg/kg BW). Transcardial perfusion was performed with 100-400 mL (bodyweight depending) cooled (4° C) 0.9% w/v NaCl-solution. After decapitation

and brain dissection, the dissected brain regions were weighed and stored at -80° C until homogenization. From pentobarbital injection to -80° C storage it took less than 5 min.

Homogenization

The extraction of proteins was performed according to published standardized protocols [26,30,31]. In the following the steps are described shortly. Proteins of each developmental stage (P7, P90, P637) were separated in six 2D-gels. For P7, P90 and P637, each gel image presents a single dissected brain region. The brain sections were incubated with (9 × probe mass (mg)) µL lysis buffer consisting of 7 M urea (Sigma, Steinheim, Germany), 2 M thiourea (Sigma), 4% w/v CHAPS (Sigma), 70 mM DTT (Sigma), 0.5% v/v Bio-Lyte Ampholytes pH 3-10 (Fluka, Buchs, Switzerland) and a mixture of protease inhibitors (Roche, Basel, Switzerland) additionally enriched with (0.1 × probe mass (mg)) µL Pepstatin A and PMSF (Fluka) and snap-frozen at -150° C. The samples were quickly thawed and transferred into a 2 mL Wheaton potter (neo-lab, Heidelberg, Germany) for homogenization. In the next step, glass beads (0.034 × Vtotal µl) (Roth, Karlsruhe, Germany) were added to the suspension, following a 15 s sonication, 15 s vortexing (repeated six times) and finished by shock freezing the suspension at -150° C. After fast thawing the samples, they were put in a beaker on a magnetic stirrer that was filled with ice water for 15 min. Finally, the samples were centrifuged at 17,860× g for 20 min at 4° C. The supernatant was very carefully removed using a 2 mL syringe (Becton Dickinson, Heidelberg, Germany) with a 0.5 × 25 mm needle (Becton Dickinson), because of a thick lipid coverage derived from myelinated nerve fibers. The protein concentration of the supernatant was determined by the Bradford assay.

Two dimensional polyacrylamide gel electrophoresis (2DE) rehydration

The first dimension was performed in a PROTEAN IEF cell system (Bio-Rad, Berkeley, CA, USA). Protein extracts of 1 mg protein were loaded on immobilized pH 3–10 nonlinear gradient strips with a length of 17 cm (GE-Healthcare, Buckinghamshire, UK; Art.: 17-1235-01) and actively rehydrated with 300 µL rehydration buffer consisting of 6 M urea (Sigma), 2 M thiourea (Sigma), 2% w/v CHAPS (Sigma), 16 mM DTT (Sigma), 0.5% v/v Bio-Lyte Ampholytes pH 3-10 (Fluka) at 50 V for 12 h at 20° C.

First dimension: isoelectric focusing

After rehydration, to reduce artifacts, electrode wicks (Bio-Rad) were added. Focusing started with the "conditioning step" (2 h) which subdivides into two sub-steps: (a) linear voltage rise to 500 V, step-hold 30 min; (b) linear voltage rise to 2500 V, step-hold 1 h. After that, the "slow voltage ramping" (2.5 h): quadratic voltage rise to 8000 V and the "final focusing": actual process of focusing (duration: 50.000 Vhrs) was performed. During the whole IEF the temperature was constantly kept at 20° C. After focusing the strips were stored at -80° C.

Second dimension: polyacrylamide gel electrophoresis

Focused IPG-strips were equilibrated in two steps of 30 min each in 5 mL of freshly prepared SDS equilibration solution consisting of 1.5 M Tris-HCl pH 8.8 (Roth), 6 M urea (Sigma), 30% v/v glycerol (Sigma), 2% w/v SDS (Sigma), trace of bromophenol blue (Roth) supplemented with 10 mg/mL DTT and 40 mg/mL iodoacetamide. The strips were transferred on 12% v/v homogeneous self-cast sodium dodecyl sulfate polyacrylamide gels (200 × 250 × 1.5 mm). At 125 V per gel (Power Pac 1000, Bio-Rad), they were run in the PROTEAN Plus Dodeca Cell
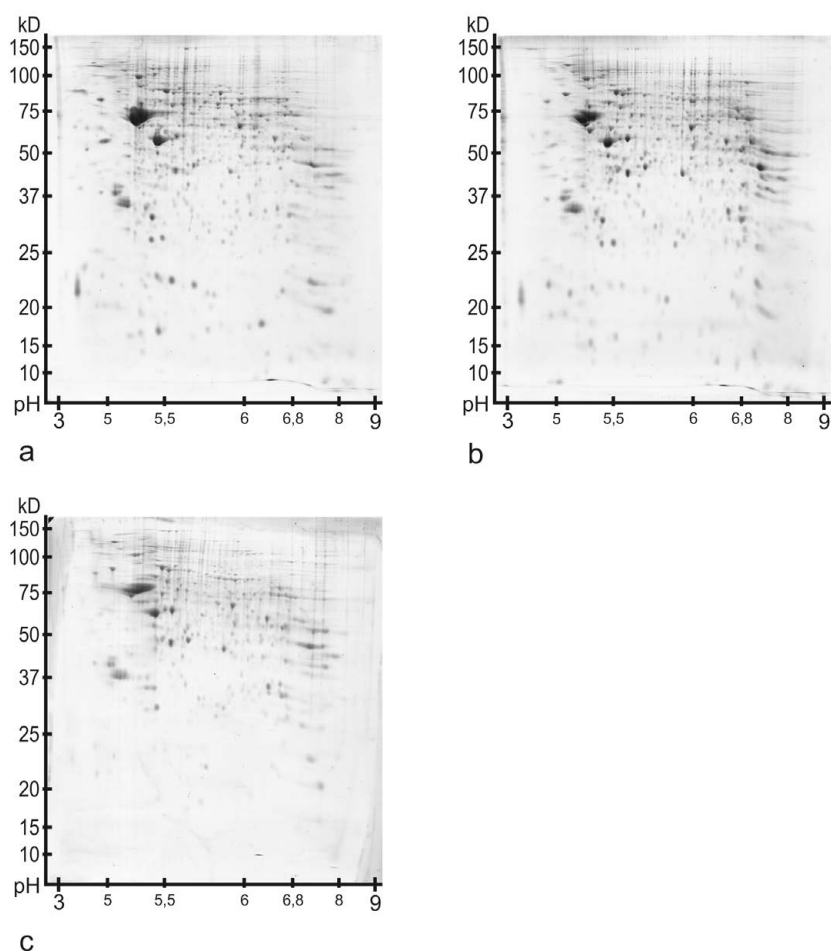
Figure 2: Overview of the reference gel images from the Cx. The coomassie blue stainings of the gels have similar intensities. (a) The 2DE-gel image of a P7 animal. (b) The 2DE-gel image of a P90 animal is presented. (c) Image of a 2DE-gel of an aged P637 rat.

(Bio-Rad). To ensure a constant buffer-temperature of 10° C, a cooling device (Julabo F10, Julabo Labortechnik, Seelbach, Germany) was used.

Fixation and staining

Fixation was performed with acetic acid-methanol solution (45% v/v methanol, 1% v/v acetic acid) overnight. Staining of the gels was performed in a colloidal CBB G250 solution (1 g/1000 mL) (Roth) as described previously [32,33]. After 24 h, the gels were destained with ultrapure water and were held in cold storage (4° C) with ultrapure water until digitization.

Gel analysis

Digitization: The stained gels (n=6) were scanned in transparence mode as 12 bit gray scale tif-images with a F4100 scanner (Heidelberg, Heidelberg, Germany) at 300 dpi resolution. Gels were rinsed in 0.02% w/v sodium azide (Aldrich Chemie, Steinheim, Germany), shrink-wrapped in plastic and stored at 4° C until picking for MALDI-TOF-MS (Figure 2).

Digital gel processing: For 2DE-gel image analysis, the software package Progenesis PG200 Version 2006 (Nonlinear Dynamics Ltd., Newcastle upon Tyne, UK) was used. The gels were registered to a reference gel (the gel which contained most spots with optimal separation and staining quality and least artifacts) and manually edited

spots (Figure S1) were matched to allow comparability of all gels (Figures 2-3).

Determination of differentially abundant protein spots

Protein spots in 2DE were quantified by normalizing spot volumes using Progenesis PG200 (Nonlinear Dynamics Ltd., Newcastle upon Tyne, UK) and spot volume differences were calculated. After the comparison of the normalized gray value-spot volumes of all generated spot pairs with Access and Excel (Windows, Microsoft Corporation, Redmond, WA, USA), the comparison of the spot volumes was determined by calculation of the spot volume quotient (SVQ, P90/P7 or P90/P637).

Only those spots were considered to be significantly up- or down-regulated that showed a SVQ (Spot Volume Quotient) of 0.6 or less and 1.67 or greater [26,31,34]. The differences were evaluated significantly if differentially expressed spots were detected in at least four gel images (correlated spots) belonging to one test group. If multiple spots of one protein were detected by mass spectrometric analysis, the differential abundance was determined by the mean of their individual abundance levels. Additionally, each protein existing in a mixed spot with at least another protein in one developmental stage was marked individually as well as if one protein was present in multiple spots per stage (Table S1). The classification of the differentially expressed proteins in their respective functional protein groups itself was generated by a
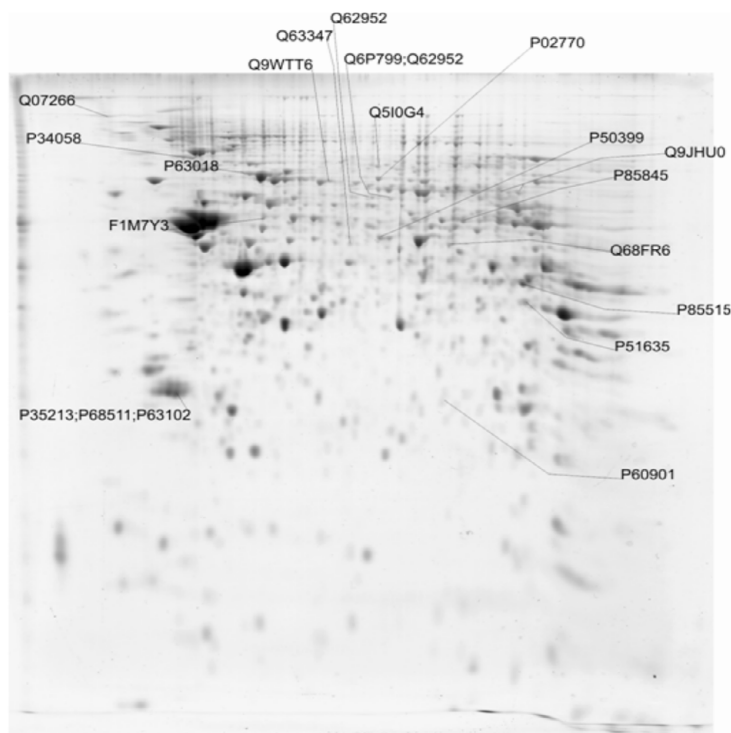
Figure 3: Differential abundance of proteins of P7 in comparison to P90. Search of proteins was performed against the Swiss Prot database. Annotation of accession numbers are from Swiss Prot in the reference gel (P90, Co reference gel: 61064). Protein mixes and multiple protein presentations in different spots can be derived from branching lines. Black: upregulated proteins. See also supplemental figures S2-S4 with differential abundance of P90 in comparison to P7, P637 in comparison to P90 and P90 in comparison to P637.

comparison of the proteins' properties; in addition, the basic function of each protein is briefly described.

Bioinformatics analysis

Histological mapping and 3D reconstructions of the rat cerebral cortex were realized in *neuroVIISAS* (http://neuroviisas.med.uni-rostock.de). Diagrams were generated with Excel 2013 (Microsoft). 2D-gel image and spot analysis was performed with Progenesis PG200 (shown above). Differentially proteins were subjected to bioinformatics analysis for protein identification (Entrez Gene: https://www.ncbi.nlm.nih.gov/gene/) and UniProtKB/Swiss-Prot (http://www.uniprot.org) as well as UniProtKB/TrEMBL). Classification of differentially proteins was done by using GeneCards (http://www.genecards.org/) and PANTHER (http://www.panther-db.org). The visualization of intergroup relations was done with a Venn diagram (http://bioinformatics.psb.ugent.be/cgi-bin/liste/Venn/calculate_venn.htpl). The pathway analysis was performed with consensus PathDB (http://cpdb.molgen.mpg.de/), STRING (http://string-db.org/) and Reactome (http://www.reactome.org/).

Mass spectrometric analysis of protein spots

Following published standardized protocols [35], protein spots were excised from the gels with a spot picker (Flexys Proteomics picker, Genomic Solutions, Ann Arbor, MI, USA), transferred into 96-well plates, and subjected to in-gel digestion with trypsin. The gel plugs were washed twice with 30% acetonitrile (ACN) in 25 mM ammonium bicarbonate and 50% ACN in 10 mM ammonium bicarbonate, respectively, shrunk with ACN, and dried at 37° C. The dried gel plugs were re-swollen with 5 µL protease solution (sequencing grade trypsin,

10 ng/µL in 3 mM Tris–HCl, pH 8.5, Promega, Madison, WI, USA) and incubated for 8 h at 37° C. Thereafter, 5 µL of extraction solution (0.3% trifluoroacetic acid, 50% ACN) were added and the samples were agitated at room temperature for 30-60 min before the peptide extracts were transferred into the 96-well collection plates. The resulting peptide-containing solution was prepared for MALDI analysis by spotting 0.6 µL of the tryptic digest and 0.45 µL of matrix solution consisting of 9 mg/mL α-cyano-4-hydroxy-cinnamic acid (CHCA) in 50% ACN, 0.1% trifluoroacetic acid on standard stainless steel MALDI plates. MALDI-MS analysis was performed on a 4700 Proteomics Analyzer MALDI-TOF/TOF mass spectrometer (Applied Biosystems, Foster City, CA, USA). All acquired spectra were processed using 4700 Explore™ software (Applied Biosystems, Warrington, Cheshire, UK). For protein identification, spectra were submitted to MASCOT (version 2.4.0, Matrix Science, London, UK) via the MASCOT Deamon. Searches were performed against the subset of rat proteins of the UniProtKB protein sequence database (2012_01; 42755 sequences from Rattus). A mass tolerance of 60 ppm and one missing cleavage site were set, oxidation of methionine residues was considered as variable modification, and carbamidomethylation of cysteines as fixed modification. Peptide masses of trypsin autoproteolysis products and matrix-derived peaks were excluded. Identifications with Mascot scores greater than 59 were considered significant ($p < 0.05$). All results were examined carefully for reliability and occurrence of multiple proteins in the same sample. The search was first restricted to proteins from Rattus and thereafter repeated for rodent proteins to include proteins still missing in the sequence data of Rattus. Entries from TrEMBL were used only, if no homologous protein was contained in Swiss-Prot or if a higher number of peptides matched to a sequence from the TrEMBL database.

Immunoblot analysis

The homogenated protein samples of the Cx were dissolved in sample buffer (1/1 dilution with 2x SB). For immunoblotting, total cellular extracts (30 µg per lane) were separated by SDS-Page using 4-20% polyacryamide gels (Bio-Rad, Munich, Germany) and transferred to PVDF membranes (0.2 mm, Bio-Rad, Munich, Germany). The blots were blocked with 5% non-fat dry milk powder in TBS for 30-60 min and incubated with the individual primary antibodies. The following antibodies were used (dilutions are given in the brackets): rabbit polyclonal anti-PARK 7/DJ-1 (1:800, Abcam, Cambridge, UK), rabbit polyclonal anti Drebrin (1:1000, Abcam, Cambridge, UK), mouse monoclonal anti neurofilament 68 (1:400, Sigma-Aldrich, St. Louis, Missouri, USA), mouse monoclonal anti neurofilament 160/200 (1:1000, Sigma-Aldrich, St. Louis, Missouri, USA), rabbit polyclonal anti α-Internexin (1:1000, Merck Millipore, Darmstadt, Germany). After washing, membranes were incubated with secondary HRP-conjugated anti-mouse (1:2000) and anti-rabbit (1:2000) IgG, and visualized by the Enhanced Chemiluminescence (ECL) (Lumixx plus 250) procedure as described by the manufacturer (Biostep GmbH, Burkhardtsdorf, Germany). For the molecular marker, the Precision plus Protein All Blue Standard (Bio-Rad Laboratories, Inc., Hercules, USA) was used. The analysis of the Western Blot protein signals was performed and recorded by using the Proxima 2850, CL and UV fluorescence/chemiluminescence system (Biostep GmbH,

Burkhardtsdorf, Germany) including its analysis software (ProXima AQ-4, Ref. 1.28/CLIQS, version 1.1).

Results

Identification of proteins

As described before, the 2D-PAGE method was performed for the protein separation of the Cx and its different ages (P7, P90, P637) followed by digital gel analysis ("gel-matching", "spot-warping") and a differential spot analysis combined with a protein identification (MALDI-TOF) to determine differences in the protein abundance during development and aging.

In Figure 2, the images of the reference gels of the different developmental stages are presented ((a) P7, (b) P90 and (c) P637). The spot compositions proved to be comparable. On average, 740 (±57) spots were detected in the six gels of P7, 729 (±50) spots in the gels of P90 and 488 (±43) spots in the gels of P637. An example of the manual spot editing (segmentation, delineation) by using a gel image of the Cx in Progenesis PG200 is documented in supplemental Figure S1.

In addition, the differential expressed proteins were classified into 13 functional protein groups.

In the next section, an overview of the up- and downregulation of the different protein groups within each developmental stage (P7, P637)

Accession	Entry name	Gene name	Funct. Group/Protein Name	Regulation [P7]	Regulation [P637]	Cell. Localisation
			Proteins Carbohydrate Metabolism	(SVQ ≤ 0.6)	(SVQ ≥ 1.67)	
P51635	AK1A1_RAT	Akr1a1	Alcohol dehydrogenase [NADP(+)]	up	-	Cts, M
P07943	ALDR_RAT	Akr1b1	Aldose reductase	down	-	Cp
P09117	ALDOC_RAT	Aldoc	Fructose-bisphosphate aldolase C	-	up	Cp, Mito, A
P08461	ODP2_RAT	Dlat	Dihydrolipoyllysine-residue acetyltransferase component of pyruvate dehydrogenase complex, mitochondrial	down	-	Mmt
Q01205	ODO2_RAT	Dlst	Dihydrolipoyllysine-residue succinyltransferase component of 2-oxoglutarate dehydrogenase complex, mitochondrial	down	down	Mito
P04764	ENOA_RAT	Eno1	Alpha-enolase	down	up	Cp, M
P07323	ENOG_RAT	Eno2	Gamma-enolase	down	-	Cp, M
P04797	G3P_RAT	Gapdh	Glyceraldehyde-3-phosphate dehydrogenase	down	-	Cp, Nc
P42123	LDHB_RAT	Ldhb	L-lactate dehydrogenase B chain	down	-	Cp
O88989	MDHC_RAT	Mdh1	Malate dehydrogenase, cytoplasmic	down	-	Cp
B1WC26	B1WC26_RAT	Nans	N-acetylneuraminic acid synthase	down	down	Cp, Cts
P26284	ODPA_RAT	Pdha1	Pyruvate dehydrogenase E1 component subunit alpha, somatic form, mitochondrial	down	-	Mmt
P49432	ODPB_RAT	Pdhb	Pyruvate dehydrogenase E1 component subunit beta, mitochondrial	down	-	Mmt
P25113	PGAM1_RAT	Pgam1	Phosphoglycerate mutase 1	down	-	Nc, Cts
P16617	PGK1_RAT	Pgk1	Phosphoglycerate kinase 1	down	down	Cp
P11980	KPYM_RAT	Pkm2	Pyruvate kinase isozymes M1/M2	down	-	Cp, Nc
B2RZ24	B2RZ24_RAT	Pkm3	Succinyl-CoA synthetase beta-A chain	down	-	Mito, Mmt
P48500	TPIS_RAT	Tpi1	Triosephosphate isomerase	down	-	Nc, Cts
Q68FY0	QCR1_RAT	Uqcrc1	Cytochrome b-c1 complex subunit 1, mitochondrial	down	-	Mim
			Proteins Amino Acid Metabolism			
P10860	DHE3_RAT	Glud1	Glutamate dehydrogenase 1, mitochondrial	down	up	Mmt

P09606	GLNA_RAT	**Glul**	Glutamine synthetase	down	up	Cp, Mito
F1M9V7	F1M9V7_RAT	**Npepps**	Aminopeptidase puromycin sensitive	-	up	Nc, Cp
O09175	AMPB_RAT	**Rnpep**	Aminopeptidase B	-	down	Sc, Cp
Proteins Fat Metabolism						
Q5XI22	THIC_RAT	**Acat2**	Acetyl-CoA acetyltransferase, cytosolic	down	down	Cp
Q6P6R2	DLDH_RAT	**Dld**	Dihydrolipoyl dehydrogenase, mitochondrial	-	up	Mmt
P17425	HMCS1_RAT	**Hmgcs1**	Hydroxymethylglutaryl-CoA synthase, cytoplasmic	up	-	Cp
O35760	IDI1_RAT	**Idi1**	Isopentenyl-diphosphate Delta-isomerase 1	p90: abs	-	Per
P30349	LKHA4_RAT	**Lta4h**	Leukotriene A-4 hydrolase	down	-	Cp
O35264	**PA1B2_RAT**	**Pafah1b2**	Platelet-activating factor acetylhydrolase IB subunit beta	-	up	Cp
Proteins Energy Metabolism						
P15999	ATPA_RAT	Atp5a1	ATP synthase subunit alpha, mitochondria	down	down	Mim, M
P31399	ATP5H_RAT	Atp5h	ATP synthase subunit d, mitochondrial	down	down	Mito, Mim
P25809	KCRU_RAT	**Ckmt1**	Creatine kinase U-type, mitochondrial	down	down	Mito, Mim
Q66HF1	NDUS1_RAT	Ndufs1	NADH-ubiquinone oxidoreductase 75 kDa subunit, mitochondrial	down	up	Mim
Q641Y2	NDUS2_RAT	Ndufs2	NADH dehydrogenase [ubiquinone] iron-sulfur protein 2, mitochondrial	down	-	Mim
D3ZG43	D3ZG43_RAT	**Ndufs3**	NADH dehydrogenase (Ubiquinone) Fe-S protein 3 (Predicted), isoform CRA_c	down	-	Mito, Mm
P19234	NDUV2_RAT	**Ndufv2**	NADH dehydrogenase [ubiquinone] flavoprotein 2, mitochondrial	-	p637: abs	Mim
P20788	UCRI_RAT	**Uqcrfs1**	Cytochrome b-c1 complex subunit Rieske, mitochondrial	down	-	Mim
Degratory Proteins						
P60901	PSA6_RAT	**Psma6**	Proteasome subunit alpha type-6	up	up	Cp, Nc
Q63347	PRS7_RAT	**Psmc2**	26S protease regulatory subunit 7	up	-	Cp, Nc
Q63570	PRS6B_RAT	**Psmc4**	26S protease regulatory subunit 6B	-	p637: abs	Cp, Nc
Proteins Antioxidants						
Q9Z339	GSTO1_RAT	**Gsto1**	Glutathione S-transferase omega-1	down	-	Cp, Cts
P08009	GSTM4_RAT	**Gstm3**	Glutathione S-transferase Yb-3	p7: abs	-	Cp
P35704	PRDX2_RAT	**Prdx2**	Peroxiredoxin-2	down	-	Cp
O35244	PRDX6_RAT	**Prdx6**	Peroxiredoxin-6	down	-	Cp, Lyso
Q9Z0V6	PRDX3_RAT	**Prdx3**	Thioredoxin-dependent peroxide reductase, mitochondrial	down	up	Mito
Proteins Biosynthesis						
O35567	PUR9_RAT	**Atic**	Bifunctional purine biosynthesis protein PURH	-	up	Mito, Cts
Q68FR6	EF1G_RAT	**Eef1g**	Elongation factor 1-gamma	up	-	Rs, Cts
Q5I0G4	SYG_RAT	**Gars**	Glycine--tRNA ligase	up	-	Cp, Mito
Q9WTT6	GUAD_RAT	**Gda**	Guanine deaminase	up	-	Cts
Q6P799	SYSC_RAT	**Sars**	Serine--tRNA ligase, cytoplasmic	up	-	Cp
P85834	EFTU_RAT	**Tufm**	Elongation factor Tu, mitochondrial	down	-	Mito
Proteins Signal Transduction						
P59215	GNAO_RAT	**Gnao1**	Guanine nucleotide-binding protein G(o) subunit alpha	down	-	M, hGc
P54313	GBB2_RAT	**Gnb2**	Guanine nucleotide-binding protein G(I)/G(S)/G(T) subunit beta-2	down	-	M, Cp
P62994	GRB2_RAT	**Grb2**	Growth factor receptor-bound protein 2	-	up	Nc, Cp
P63086	MK01_RAT	**Mapk1**	Mitogen-activated protein kinase 1	down	-	Nc, Cp
F1M7Y3	F1M7Y3_RAT	**Rap1gds1**	RAP1, GTP-GDP dissociation stimulator 1	up	-	Cp
Proteins Regulation						
P48037	ANXA6_RAT	**Anxa6**	Annexin A6	down	-	Cp, Mel
P27139	CAH2_RAT	**Ca2**	Carbonic anhydrase 2	down	-	Cp

P45592	COF1_RAT	**Cfl1**	Cofilin-1	down	-	Nm, Cp
Q07266	DREB_RAT	**Dbn1**	Drebrin	up	-	Cp
P50399	GDIB_RAT	**Gdi2**	Rab GDP dissociation inhibitor beta	up	-	Cp, M
Q68FS4	AMPL_RAT	**Lap3**	Cytosol aminopeptidase	-	up	Cp
Q99MZ8	LASP1_RAT	**Lasp1**	LIM and SH3 domain protein 1	down	down	Cp, Csk
Q64361	LXN_RAT	**Lxn**	Latexin	down	-	Cp
O88767	PARK7_RAT	**Park7**	Protein DJ-1	down	-	Cp, Nc, Mito
P62138	PP1A_RAT	**Ppp1ca**	Serine/threonine-protein phosphatase PP1-alpha catalytic subunit	-	up	Cp, Nc
Q6AXV4	SAM50_RAT	**Samm50**	Sorting and assembly machinery component 50 homolog	down	down	Mom, Cp
P70566	TMOD2_RAT	**Tmod2**	Tropomodulin-2	down	down	Cp, Csk
Q5RKI0	WDR1_RAT	**Wdr1**	WD repeat-containing protein 1	down	-	Cp, Csk
Chaperones						
P18418	CALR_RAT	**Calr**	Calreticulin	down	down	ER
P63036	DNJA1_RAT	**Dnaja1**	DnaJ homolog subfamily A member 1	p7: abs	-	M, La
P63018	HSP7C_RAT	**Hspa8**	Heat shock cognate 71 kDa protein	up	up	Cp, Mel
P63039	CH60_RAT	**Hspd1**	60 kDa heat shock protein, mitochondrial	down	-	Mmt
Q5XHZ0	TRAP1_RAT	**Trap1**	Heat shock protein 75 kDa, mitochondrial	down	down	Mito
Structural Proteins						
P60711	ACTB_RAT	**Actb**	Actin, cytoplasmic 1	down	-	Cp, Csk
Q62950	DPYL1_RAT	**Crmp1**	Dihydropyrimidinase-related protein 1	up	-	Cp, Csk
P85845	FSCN1_RAT	**Fscn1**	Fascin	up	up	Cp, Csk
P47819	GFAP_RAT	**Gfap**	Glial fibrillary acidic protein	down	up	Cp
D4A6B2	D4A6B2_RAT	**Immt**	Mitochondrial inner membrane protein	down	-	Mito, Mim
P23565	AINX_RAT	**Ina**	Alpha-internexin	down	-	Nf
P19527	NFL_RAT	**Nefl**	Neurofilament light polypeptide	down	-	Nf, A
P12839	NFM_RAT	**Nefm**	Neurofilament medium polypeptide	down	-	Nf, Csk, A
B5DFG5	B5DFG5_RAT	**Sep-06**	Septin-6	down	-	Cr, Cp
B0BNF1	SEPT8_RAT	**Sep-08**	Septin-8	down	down	Cp, Csk
Q6AYZ1	TBA1C_RAT	**Tuba1c**	Tubulin alpha-1C chain	down	-	Cp, Csk
Transport Proteins						
P85515	ACTZ_RAT	**Actr1a**	Alpha-centractin	up	-	Cp, Cts
P02770	ALBU_RAT	**Alb**	Serum albumin	up	-	Sc
Q5M7T6	Q5M7T6_RAT	**Atp6v0d1**	ATPase, H+ transporting, lysosomal 38kDa, V0 subunit d1	down	down	M
P62815	VATB2_RAT	**Atp6v1b2**	V-type proton ATPase subunit B, brain isoform	down	-	M, Mel
P85969	SNAB_RAT	**Napb**	Beta-soluble NSF attachment protein	down	down	M
Q9QUL6	NSF_RAT	**Nsf**	Vesicle-fusing ATPase	down	-	Cp
Q9Z2L0	VDAC1_RAT	**Vdac1**	Voltage-dependent anion-selective channel protein 1	down	down	Mom, M
P81155	VDAC2_RAT	Vdac2	Voltage-dependent anion-selective channel protein 2	down	-	Mom

Table 1: Proteins identified by peptide mass fingerprinting in spots from Coomassie-stained gels arranged by their function. Accession: Accession number from UniProtKB/Swiss-Prot; Entry name: Entry name from UniProtKB/Swiss-Prot; Gene name: from UniProtKB/Swiss-Prot; Regulation (P7)/Regulation (P637): Differential abundance in comparison to P90.The full description for the cellular location is given in the list of abbreviations. SVQ: Spot volume quotient. Further parameters are shown in Table S1.

is listed and described in relation to the comparison group (P90) for the brain region of the Cx. The specific differential expressed proteins are described in detail in Table 1, in the following text they are only described in a quantitative manner.

Mass spectrometric results of cortical protein identification

At P7, 82 proteins were found which showed a difference in their abundance in comparison to P90. This includes 63 proteins which were downregulated compared to P90, whereas 16 proteins showed an upregulation. In addition, two proteins were analyzed only in P90 and, therefore, were absent at P7. One protein was absent at P90 (Table 2).

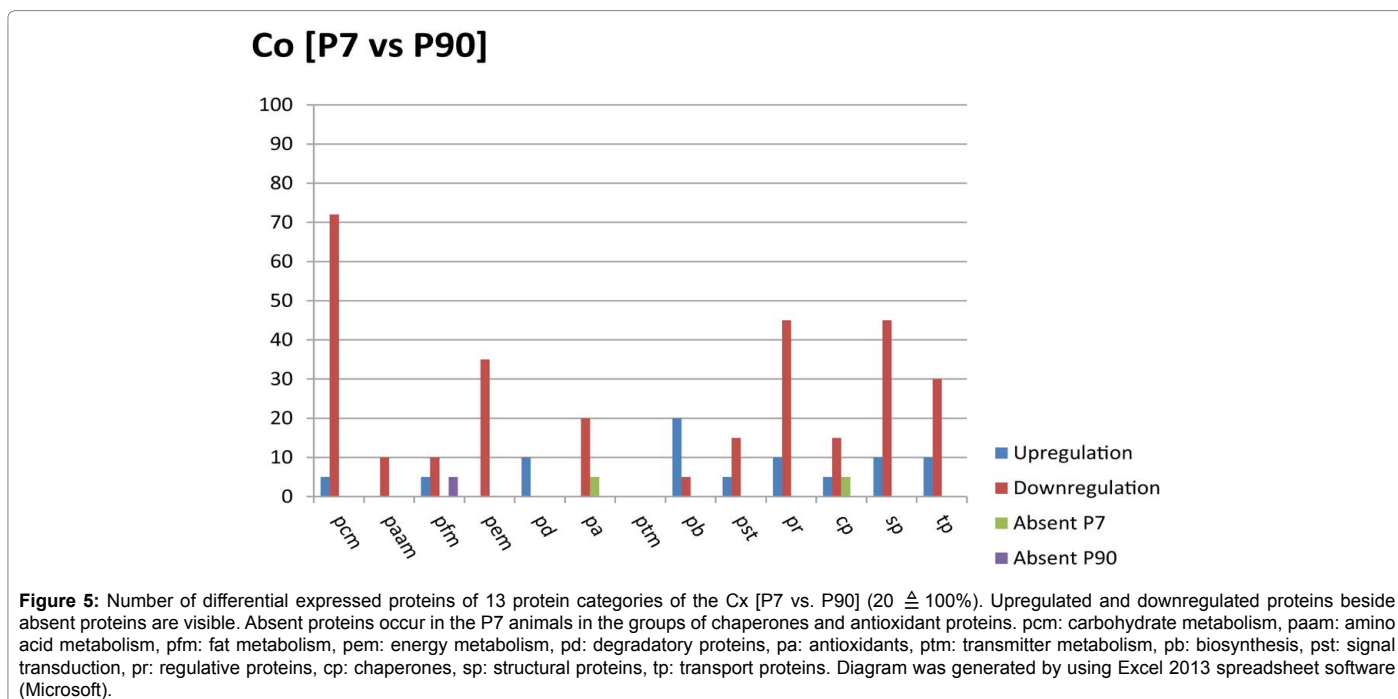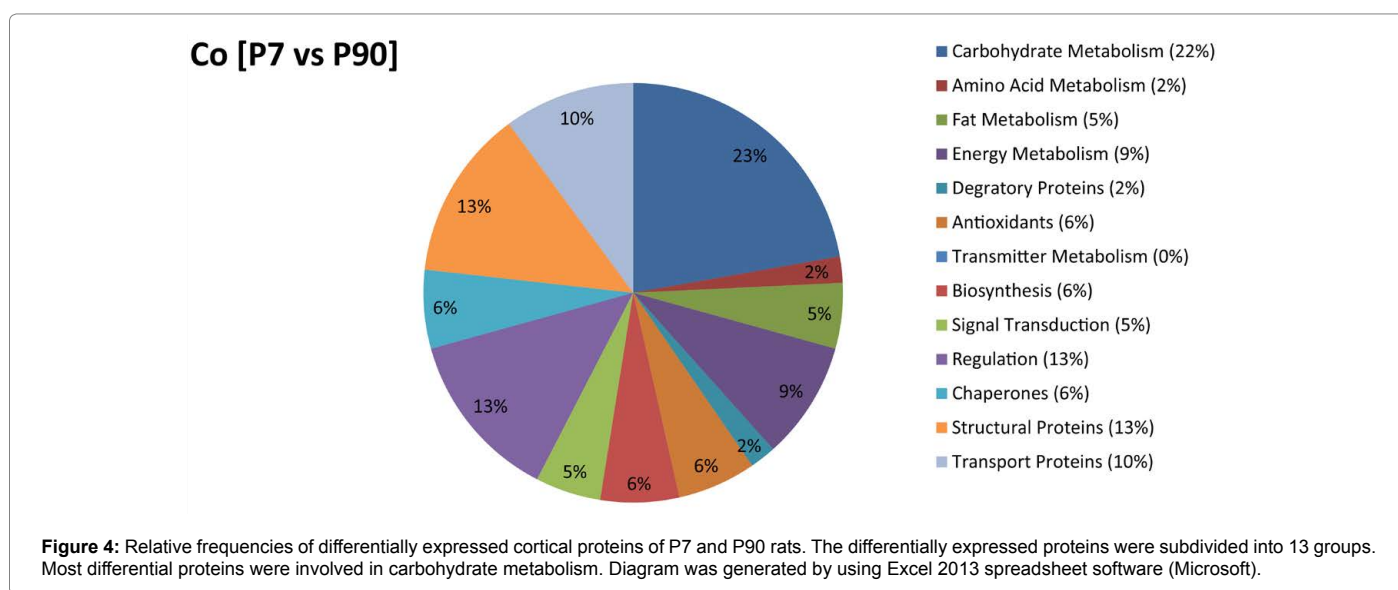## Differences in the abundance of proteins of P7 in comparison to P90

The differential abundance of upregulated proteins in P7 (P7>P90) is shown in Figure 3, whereas, upregulated proteins in P90 (P7<P90) rats are documented in supplemental Figure S2.

The largest number of differentially expressed proteins belongs to the carbohydrate metabolism (total amount: 22%) (Figure 4). 17 downregulated (P7<P90) proteins and one upregulated (P7>P90) protein of P7 compared to P90 (Figure 5) were found in this category. For example, the protein alcohol dehydrogenase (Akr1a1) which catalyzes

Category	Amount [P7] (Total value)	Amount [P637] (Total value)
Total amount	82	36
Upregulation	16	17
Downregulation	63	17
Absent	2	2
Absent P90	1	0

Table 2: Overview of the differential abundance of the proteins of the Cx in P7 and P637 in comparison to P90.

the reduction of a number of aldehydes, including the aldehyde form of glucose, and is thereby implicated in the development of diabetic complications by catalyzing the reduction of glucose to sorbitol which was upregulated at the developmental stage of P7. The protein glyceraldehyde-3-phosphate dehydrogenase (Gapdh) displays a protein which showed a downregulation in comparison to P90. This protein has both glyceraldehyde-3-phosphate dehydrogenase and nitrosylase activities and thereby plays a role in glycolysis and nuclear functions. Therefore, it is a key enzyme in glycolysis that catalyzes the first step of the pathway by converting D-glyceraldehyde 3-phosphate (G3P) into 3-phospho-D-glyceroyl phosphate. Also the protein pyruvate dehydrogenase E1 component subunit beta, mitochondrial (Pdhb) showed a downregulation at this developmental stage. It represents a member of a multienzyme complex that catalyzes the overall conversion

Figure 4: Relative frequencies of differentially expressed cortical proteins of P7 and P90 rats. The differentially expressed proteins were subdivided into 13 groups. Most differential proteins were involved in carbohydrate metabolism. Diagram was generated by using Excel 2013 spreadsheet software (Microsoft).

Figure 5: Number of differential expressed proteins of 13 protein categories of the Cx [P7 vs. P90] (20 ≙ 100%). Upregulated and downregulated proteins beside absent proteins are visible. Absent proteins occur in the P7 animals in the groups of chaperones and antioxidant proteins. pcm: carbohydrate metabolism, paam: amino acid metabolism, pfm: fat metabolism, pem: energy metabolism, pd: degradatory proteins, pa: antioxidants, ptm: transmitter metabolism, pb: biosynthesis, pst: signal transduction, pr: regulative proteins, cp: chaperones, sp: structural proteins, tp: transport proteins. Diagram was generated by using Excel 2013 spreadsheet software (Microsoft).

of pyruvate to acetyl-CoA and carbon dioxide and provides the primary link between glycolysis and the tricarboxylic acid cycle.

The structural proteins also showed a high amount of differentially expressed proteins. 13% of differentially regulated proteins belong to this class where two upregulated (P7>P90) and nine downregulated (P7<P90) proteins could be identified. For the upregulated proteins at this developmental stage, for example, the dihydropyrimidinase-related protein 1 (Crmp1) showed a higher abundance at the early developmental stage of P7 compared to P90. The protein fascin (Fscn1) was also upregulated at this stage, which organizes filamentous actin into bundles and the formation of microspikes, membrane ruffles, and stress fibers. Therefore, it is important for the formation of a diverse set of cell protrusions, such as filopodia, and for cell motility and migration. Different members of the neurofilaments were downregulated in P7, for example, the protein alpha-internexin (Ina) as well as the neurofilament light polypeptide (Nefl) and the neurofilament medium polypeptide (Nefm) which showed a higher abundance at P90 compared to P7. These different members of the neurofilaments belong to the type IV intermediate filament heteropolymers which are composed of light, medium, and heavy chains. In general, neurofilaments comprise the axoskeleton and they functionally maintain the neuronal caliber. They may also play a role in intracellular transport to axons and dendrites and their morphogenesis. Additionally, for the neurofilaments (Nefl, Nefm) this trend of abundance could be verified by Western Blot analysis (Figure 9). Also the protein actin, cytoplasmic 1 (Actb) showed a lower abundance at P7 in comparison to P90. This protein represents a member of one of the six different actin proteins. Actin members are highly conserved proteins that are involved in cell motility, structure, and integrity.

Another large differential abundance was found for the regulatory proteins (total amount: 13%). They showed a stronger tendency to downregulation (P7<P90) (nine downregulated proteins, two upregulated proteins). In this category, for example the downregulated protein annexin A6 (Anxa6) represents a member belonging to a family of calcium-dependent membrane and phospholipid-binding proteins which have been implicated in membrane-related events along exocytotic and endocytotic pathways.

Another downregulated protein in comparison to P90, Protein DJ-1 (Park7), functions as a redox-sensitive chaperone and as a sensor for oxidative stress. It can protect neurons against oxidative stress and cell death. In P7 the Rab GDP dissociation inhibitor beta (Gdi2) as well as the protein Drebrin (Dbn1) showed a higher abundance (P7>P90). While Gdi2 presents a member of GDP dissociation inhibitors which regulates the GDP-GTP exchange reaction of members of the rab family and is therefore involved in vesicular trafficking of molecules between cellular organelles, Dbn1 functions as a cytoplasmic actin-binding protein that plays a role in the process of neuronal growth. Also by Western Blot analysis the upregulation of Dbn1 at P7 in comparison to P90 could be confirmed (Figure 9).

In the remaining functional protein classes, i.e. the transport proteins (10% total amount, two upregulated (P7>P90) and six downregulated (P7<P90) proteins), the proteins of the energy metabolism (Total amount: 9%, seven downregulated (P7<P90) proteins), the chaperones (Total amount: 6%, three downregulated (P7<P90) proteins and one upregulated (P7>P90) protein, one protein was absent at P7), proteins of the biosynthesis (Total amount: 6%, four upregulated (P7>P90) and one downregulated (P7<P90) protein), antioxidant proteins (total amount: 6%, four downregulated (P7<P90) proteins, one protein absent at P7), proteins of the fat metabolism (total

amount 5%, two downregulated (P7<P90) proteins, one upregulated (P7>P90) protein, one protein is absent at P90), proteins involved in the signal transduction (total amount: 5%, one upregulated (P7>P90) and three downregulated (P7<P90) proteins), proteins of the amino acid metabolism (total amount: 2%, two downregulated (P7<P90) proteins a well as the degratory proteins (total amount: 2%, two upregulated (P7>P90) proteins), differences in the abundance of the protein categories could be determined as well. Only proteins involved in the metabolism of neurotransmitters showed no detectable differences in these ages of the brain during the analysis.

Differences in the abundance of proteins of P637 in comparison to P90

Gels documenting the differential up- and downregulation of proteins with annotated accession numbers of the time points P90 and P637 are shown in supplemental Figures S3 and S4.

Several differentially expressed proteins could be found at P637 and P90 of development. In principle, a smaller number of differentially expressed proteins were detectable as compared to P7. Taken together, a change in their abundance was observable for 36 proteins between both developmental stages. 17 proteins showed an upregulation (P637>P90), 17 proteins were downregulated (P637<P90) and two proteins were only detectable at P90, respectively they were absent at P637 (Table 2). The proteins of the energy metabolism show the most differentially expressed proteins (total amount: 14%) (Figure 6). Three proteins showed a downregulation (P637<P90), whereas one protein was upregulated (P637>P90) and one protein was absent at P637 (Figure 7). As for the two subunits of the mitochondrial ATP synthase (subunit alpha (Atp5a1), subunit d (Atp5h)) showed a lower abundance (P637<P90). Both subunits participate in the catalysis of ATP synthesis by using an electrochemical gradient of protons across the inner membrane during oxidative phosphorylation. The NADH-ubiquinone oxidoreductase 75 kDa subunit (Ndufs1) was upregulated which has NADH-dehydrogenase activity and oxidoreductase activity and transfers electrons from NADH to the respiratory chain. NADH dehydrogenase flavoprotein 2 (Ndufv2) was analyzed as absent at P637 in comparison to P90 which also functions as a subunit of the mitochondrial membrane respiratory chain NADH dehydrogenase (Complex I) that is believed to belong to the minimal assembly required for catalysis. Other functional protein classes possessing similar amounts of differentially expressed proteins (14%) were determined. Three regulatory proteins were downregulated (P637<P90) and two proteins were upregulated (P637>P90). The downregulated tropomodulin-2 (Tmod2) presents a neuronal-specific member of the tropomodulin family of actin-regulatory proteins. The protein caps the pointed end of actin filaments preventing both elongation and depolymerization, whereas the capping activity of this protein is dependent on its association with tropomyosin. The serine/threonine-protein phosphatase PP1-alpha catalytic subunit (Ppp1ca) was upregulated (P637>P90) and is needed for cell protection against oxidative stress and cell death acting as an oxidative stress sensor and redox-sensitive chaperone. This protease is also required for the correct mitochondrial morphology and its function as well as for the autophagy of dysfunctional mitochondria.

The proteins of the carbohydrate metabolism (three downregulated proteins and two upregulated proteins) showed the same amount (14%) of differentially expressed proteins at this developmental stage. Phosphoglycerate kinase 1 (Pgk1) showed a downregulation (P637<P90). It catalyzes the conversion of 1.3-diphosphoglycerate to 3-phosphoglycerate within the glucose metabolism. Fructose-
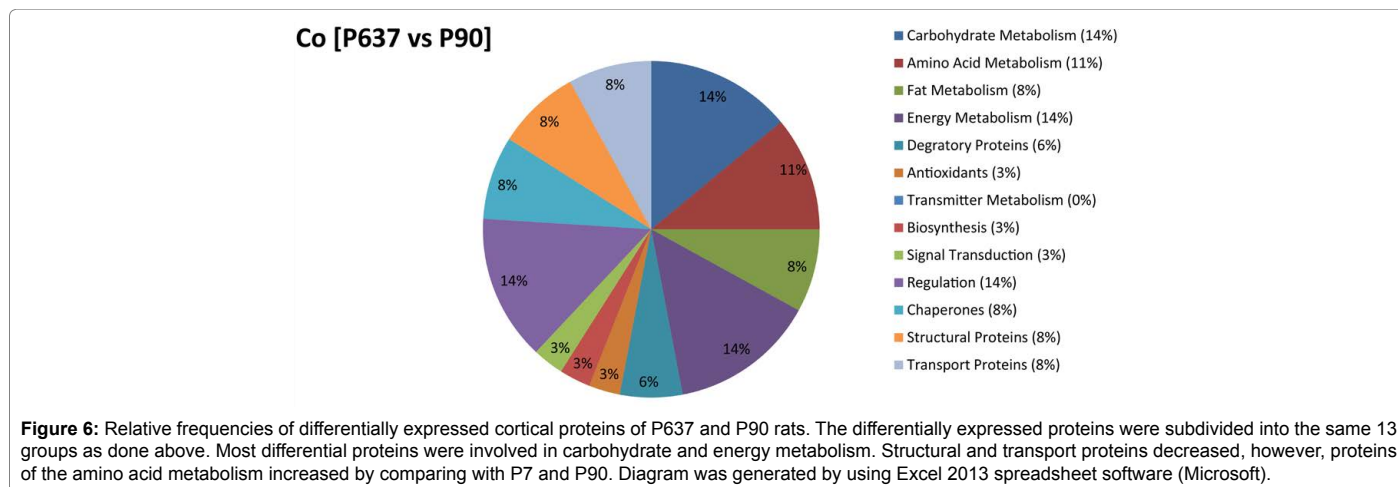
Figure 6: Relative frequencies of differentially expressed cortical proteins of P637 and P90 rats. The differentially expressed proteins were subdivided into the same 13 groups as done above. Most differential proteins were involved in carbohydrate and energy metabolism. Structural and transport proteins decreased, however, proteins of the amino acid metabolism increased by comparing with P7 and P90. Diagram was generated by using Excel 2013 spreadsheet software (Microsoft).
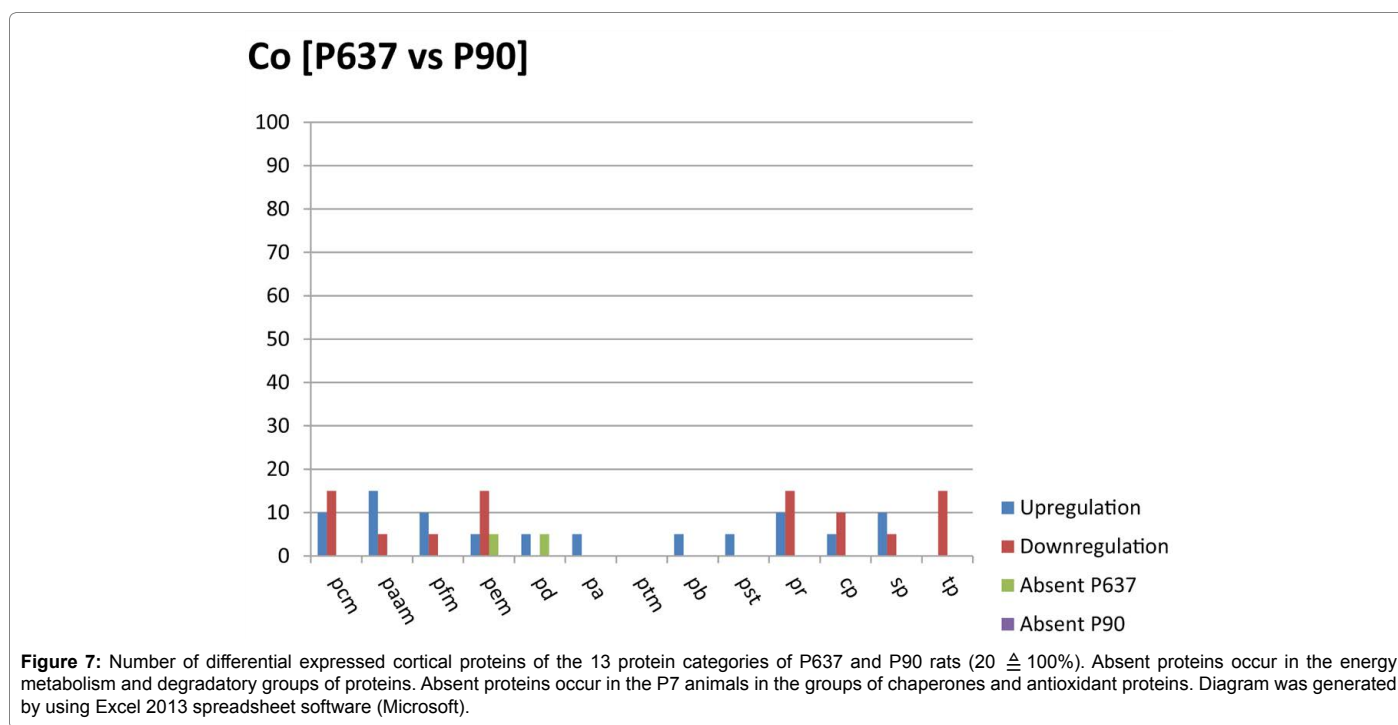

Figure 7: Number of differential expressed cortical proteins of the 13 protein categories of P637 and P90 rats (20 ≙ 100%). Absent proteins occur in the energy metabolism and degradatory groups of proteins. Absent proteins occur in the P7 animals in the groups of chaperones and antioxidant proteins. Diagram was generated by using Excel 2013 spreadsheet software (Microsoft).

bisphosphate aldolase C (Aldoc) was upregulated (P637>P90). It shows a relatively strong abundance in the hippocampus and in cerebellar Purkinje cells. It represents a glycolytic enzyme that catalyzes the reversible aldol cleavage of fructose-1.6-biphosphate and fructose 1-phosphate to dihydroxyacetone phosphate and either glyceraldehyde-3-phosphate or glyceraldehyde. Alpha-enolase (Eno1) showed a stronger abundance signal (P637>P90). It is a multifunctional enzyme that takes part in glycolysis, growth control, hypoxia tolerance and allergic responses.

Within the amino acid metabolism (total amount 11%), three upregulated (P637>P90) and one downregulated (P637<P90) proteins were found. Furthermore, the proteins of the fat metabolism (total amount: 8%) showed two upregulated (P637>P90) and one downregulated (P637<P90) protein. The same amount of differentially expressed proteins could also be determined within the group of transport proteins (three downregulated (P637<P90)

proteins), the structural proteins (one upregulated (P637>P90) and two downregulated (P637<P90) proteins) as well for the chaperones (one upregulated (P637>P90) and two downregulated (P637<P90) proteins). The proteins which are involved in degratory processes (total amount: 6%, one upregulated (P637>P90) protein, one protein was absent in P637), proteins of the signal transduction (total amount: 3%, one upregulated (P637>P90) protein) as well as the proteins with antioxidant properties (Total amount: 3%, one upregulated (P637>P90) protein) and the proteins of the biosynthesis (total amount: 3%, one upregulated (P637>P90) protein) also showed a differential abundance, but to a lesser extent.

In the set or Venn diagram (Figure 8) differentially expressed proteins were identified that share different experimental groups. The three upregulated proteins Psma6, Hspa8 and Fscn1 are upregulated in the P637 and P7 group in relation to P90. In both groups six differentially expressed proteins that are downregulated in P7, however, upregulated in P637 with regard to P90 could be identified: Ndufs1,

Prdx3, Glud1, Eno1, Gfap, Glul. 16 differentially expressed proteins that are downregulated in the P7 as well as in the P637 group with regard to the P90 rats were found: Acta2, Atp6v0d1, Samm50, Lasp1, Nans, Atp5h, Calr, Sep08, Atp5a1, Napb, Dlst, Pgk1, Ckmt1, Trap1, Tmod2, Vdac1.

Western blot validation

Five exemplary proteins with differential abundances in ages of the brain P7, P90 and P637 were validated using Western Blot analysis, since this method is one possibility to verify the proteome.

The structural proteins α-Internexin (Ina), the neurofilaments (neurofilament medium polypeptide (NF-M, Nefm), neurofilament light polypeptide (NF-L, Nefl)) and the regulatory protein DJ-1 (Park7) were downregulated (P637<P90) in the Western Blots (Figure 9). The precise values for the abundance changes (band volumes) can be found in Supplemental Table S2.

Drebrin (Dbn1) was upregulated at P7 (P7>P90) which was confirmed by the Western Blot. On the basis of Figure 9, especially the band between 75 kDa and 150 kDa (red circle, Figure 9) showed a stronger signal compared to the lanes of P90 and P637, whereas the Dbn1 antibody used, typically detects a signal with a molecular weight of 65 kDa for this protein. A possible explanation for the additionally detected bands could be a result due to the large number of negatively charged residues in this protein.

Discussion

The postnatal development and aging of the cerebral cortex (Cx) of the laboratory rat (Figure 1) can be quantified on the level of mRNA, immunohistochemical detection of proteins, histochemical and chemoarchitectonis as well as macroscopic small animal MRI studies. Here, we investigated the development and aging of the cortical proteome by gel electrophoresis and analytical mass spectrometry to reveal differentially expressed proteins during postnatal P7 (juvenile), P90 (adult) and P637 (aged) laboratory rats. An insight into the development of the postnatal development of the cortical connectome may offer new targets for genetherapy and transplantation of progenitor cells for neurodegenerative diseases.

The proteome of the cerebral cortex (Cx) of the laboratory rat (Figure 1) was analyzed by mass spectrometry at different dates of development (postnatal P7 (juvenile), P90 (adult), P637 (aged)) to determine those proteins that are differentially expressed during significant stages of postnatal development and aging. Proteins which are involved in processes of proliferation, migration and differentiation were of particular interest. The analysis should contribute to a better understanding and characterization of the proteome development of whole tissue preparation including the microenvironment. The knowledge of differentially expressed proteins could support the successful transplantation of progenitor cells in models of neurodegenerative diseases.

The Cx does not consist of a homogeneous cell population (neurons, glia and other cell population, extracellular matrix, neuropil). Protein abundance of cells and ECM of different cortical regions overlap in the gels. Therefore, a proteomic analysis of this large part of the brain also displays protein changes of non-neural cell populations and neuropil besides the differentially expressed proteins of the neural cells. In addition, using the method applied in this study also involves certain limitations, for example, a protein separation within the range of approximately 10-100 kDa and between a pH-range of 3-10. Hence, it is possibe to analyze a high percentage of the proteome of the Cx, but not its full composition. As shown in Figure 2, it is observable that especially the lateral parts of the gels show a lower resolution than the central parts which can lead to a possible misinterpretation of the regulation analysis of some protein spots.

Therefore, it is possible to analyze a major part, but not the entire proteome of the Cx [36]. Additionally, it has to be mentioned that no analysis of enzyme activity was performed in this study. The enzymatic activity of the specific proteins which can be influenced by factors like the substrate availability or the surrounding pH-value, for example, are beyond the scope of this investigation [26].

Furthermore, it is known that some proteins may be compromised in multiple spots within different locations in gels which can be a reason for different posttranslational modifications and isoforms of the same protein. As a result, a particular spot of a single protein may only show an average change of the spot volume but this does not concurrently apply for a specific protein of such a mixture of proteins within the same spot. However, with additional mass spectrometric detection methods
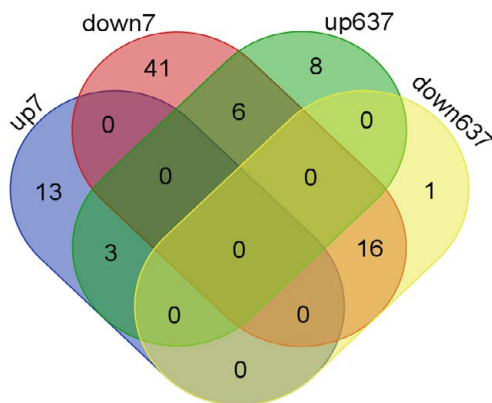

Figure 8: This Venn diagram shows the logical relations between the differentially proteins of all experimental groups. The number proteins that show differences in two groups are indicated by overlapping regions. up7: number of upregulated proteins in the P7 group in relation to the P90 group. down7: number of downregulated proteins in the P7 group in relation to the P90 group. up637: number of upregulated proteins in the P637 group in relation to the P90 group. down637: number of downregulated proteins in the P637 group in relation to the P90 group.
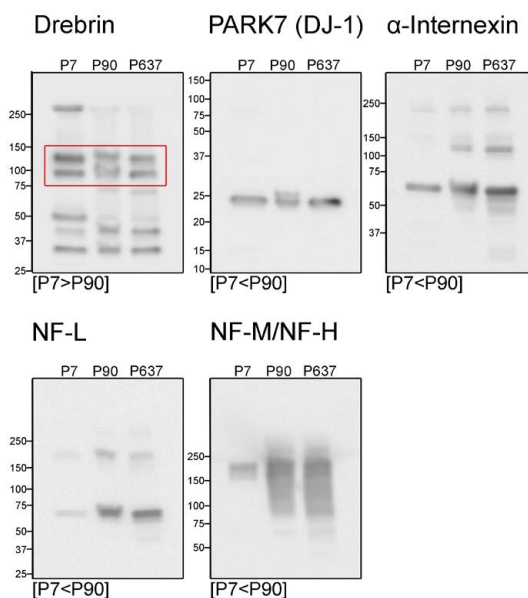
Figure 9: Validation of single differentially expressed proteins of the Cx with Western Blot analysis (rabbit polyclonal anti Drebrin, rabbit polyclonal anti-PARK 7/DJ-1, rabbit polyclonal anti α-Internexin, mouse monoclonal anti neurofilament 68, mouse monoclonal anti neurofilament 160/200, between the developmental stages (P7, P90 and P637). Differential abundances of proteome analysis are shown in brackets.

like the stable isotope ratio mass spectrometry (SIRMS) it would be possible to identify both the protein and its variants more precisely and to overcome the sample-to-sample recovery variabilities associated with non-SIRMS MS-proteomic methods. Also an improved analysis of the lower expressed and abundant proteins would be allowed by using affinity-enrichment-MS methods and targeted biomarker discovery applications (e.g. IDBEST™, iTRAQ™) [37]. The UniProtKB protein sequence database in the version of 2012_01 with 42755 sequences from Rattus has been used. An update of the search could reveal further aspects of identified proteins. However, the search was first restricted to proteins from Rattus and thereafter repeated for rodent proteins to include proteins still missing in the sequence data of Rattus. Hence, entries from TrEMBL were used only, if no homologous protein was contained in Swiss-Prot or if a higher number of peptides matched to a sequence from the TrEMBL database.

Therefore, two databases should provide a reliable identification of the proteins that were found in this study. The results of this study which deals with the proteomic analysis of the Cx of the rat can be seen as a first step to obtain an overview of the differentially expressed proteins in this multiarea part of the laboratory rat prosencephalon.

Proteins exhibit changes of abundance in independent samples at significant developmental stages of the Cx. The different abundance levels of the proteins were determined and the changes were compared with findings in the literature. In general, specific changes in the abundance of cytoplasmatic proteins in the postnatal development of the Cx were identified.

Abundance changes of proteins of the carbohydrate metabolism of P7 and P90 are relatively strong. At P637, mainly proteins of the energy metabolism, regulatory proteins and proteins participating in carbohydratic processes demonstrated the highest abudance of differentially expressed proteins. These findings suggest that the above mentioned categories of proteins are important for the development of the rat brain, for example, for the maintenance of the cytoskeleton and the energy metabolism of the rat Cx.

Most of the proteins of the carbohydrate metabolism (total amount of differentially expressed proteins: P7 vs. P90: 22%; P637 vs. P90: 14%) at the developmental stage P7 are involved in the tricarboxylic acid cycle and glycolysis. Almost all of these differentially expressed proteins show a downregulation at the early stage of P7 compared to P90. For example, the proteins gamma- and alpha enolase (Eno1, Eno2) are downregulated towards P90. While Eno1 presents a multifunctional enzyme that, besides having its functional role in glycolysis, plays a part in various processes such as growth control, for example, Eno2 catalyzes the conversion of 2-phosphoglycerate to phosphorenolpyruvate and which also has neuroprotective properties [38]. Already Wilbur and Patel [39] described the activities of several proteins involved in the tricarboxylic acid cycle and pyruvate metabolism showing low abundance levels in newborn rats, whereas they are increased markedly to adult levels during 10-30 postnatal days but do not decrease in adulthood. Also other members of this group like phosphoglycerate kinase 1 (Pgk1) and its isoenzymes (pyruvate kinase isozymes M1/M2 (Pkm2)) participate in glycolysis and show a downregulation (P7<P90). The sole upregulated protein in this category (alcohol dehydrogenase (AKR1A1)) is a member of proteins which catalyze the reduction of mevaldate to mevalonic acid and of glyceraldehyde to glycerol and are also involved in a variety of aromatic and aliphatic aldehydes to their corresponding alcohols. Further, differentially regulated proteins which are directly involved in various steps of the carbohydrate metabolism (e.g. aldose reductase (Akr1b1), pyruvate dehydrogenase E1 component subunit alpha (Pdha1), and pyruvate dehydrogenase E1 component subunit beta (Pdhb)) could be identified. Summarizing, carbohydrate proteins show a tendency to a lower abundance at P7 in comparison to P90. This juvenile (P7) carbohydrate downregulation could be the outcome of a postnatal recreation. The placenta supplements of the rat's mother seem to deliver sufficient supplies for the carbohydrate metabolism of the juvenile rat brain. After birth, maternal feeding also provides enough glucose, lactate and ketone bodies for the juvenile metabolism. Within P5 the

rat exhibits the highest ketone body concentration which subsequently decreases up to P30 [40]. By the change of the energy substrate in the adult animal, a higher abundance of proteins which are important for the metabolism of glucose is known [41]. Under normoxic conditions, the scope of glucose uptake accounts for one fifth of the amount in the adult animal [42]. Also Wilbur and Patel [39] were able to demonstrate that different proteins involved in the tricarboxylic acid cycle and the pyruvat metabolism show a lower abundance level in newborn rats. Whereas these abundance levels increase between postnatal days P10-P30, a reduction of the abundance is not detectable. Partly, for some of the proteins of the glucose metabolism an upregulation was also detectable between P90 and P637. An explanation for this could be the reduction of the metabolisation of glucose at the higher age which can lead to an impairment of performing cognitive tasks. An upregulation of these proteins can present an indication for the reaction of the animal to maintain physiologic basic states and, therefore, to produce enough energy for the neural integrity of the animal.

Major differences in the differential abundance of structural proteins between P7 and P90 were found (total amount of differentially expressed proteins: P7 vs. P90: 13%; P637 vs. P90: 8%). Most structural proteins are cytoskeletal components which are indispensable for the highly complex morphologies of dendritic and axonal arbors, which are developing in this period. This concerns the dynamic organization of the cytoskeleton [43], the axonal and the dentritic expansion as well as the establishment of synaptic contacts [44-46]. The gene of beta-Actin (Actb) (P7<P90) encodes one of six different actin proteins. Actins are highly conserved proteins that are involved in cell motility, structure, and integrity. The determined differential abundance could be explained by the associated dynamic intracellular mechanism of this protein. The protein can be found in two different forms in the cell: G-actin describes the globular monometric form, whereas F-actin forms helical polymers. Both forms present flexible structures which have important roles inside dynamic, regulated actin-networks [47]. The protein has the capability of four main functions in this network: the composition of microfilaments by forming polar rails for kinesin motorproteins (for the vesicle and organelle transport), as a component for the cytoskeleton, influencing the cell motility by (de-) polymerisation of fibrils, as well as the connection of myosin for the generation of the actomyosin complex.

Members of the septin protein family show a differential regulation within the determined developmental stages. These proteins present GTP-binding macromolecules which are involved in the control and regulation of cellular processes to synthesize filaments. As described in other sources, because of their filamentous organization as well as their association with cell membranes, actin filaments and microtubles these proteins are referred to as cytoskeletal components. In general, septin filaments show no polar formation, but their composition is comparable to the formation of intermediary filaments [48].

The protein septin-6 (Sept6) shows a downregulation at the developmental stage P7 compared to P90. Septin-8 (Sept8) is downregulated at P7 and also exhibits a downregulation at P637 compared to P90. The findings suggest a high occurrence of the expression of these proteins at the developmental stage P90. As stated before, because of the differential regulation of the different members of this protein family combined with their dynamic properties, e.g., the impact of dendritogenesis and axogenesis [49], this may give an indication for their differential abundance.

Furthermore, different members of the neurofilament family with

a differential abundance between the investigated developmental stages could be found. The proteins neurofilament light polypeptide (Nefl) as well as neurofilament medium polypeptide (Nefm) show a downregulation (P7<P90). This observation was confirmed by Western Blot analysis (Western Blot validation (Figure 9)). The neurofilaments belong to the type IV intermediate filaments which are classified in light, medium and heavy chain proteins. Functionally, these proteins play a major role in axonal growth, neuronal polarity and axonal signal transduction [50]. As described by Riederer et al. [51], differences in the regulation can occur during the ontogenesis, whereas a distinction has to be made between different cell types and their abundance. In the cerebellar cortex of cats afferent mossy fibres and climbing fibres express Nefl and Nefm at the time of birth. However, in other cell types a different abundance of these proteins was observed. For example, the axons of basket cells express these proteins one month postnatal. Relatively late, Nefl and Nefm are expressed in parallel fibres, detectable at the beginning of the third month after birth. Therefore, this study can provide an idea why the proteins show a higher differential abundance after P7, whereas no differentiation is found between the different compartments.

The protein dihydropyrimidinase-related protein 1 (Crmp1) as well as the protein fascin (Fscn1) are upregulated (P7>P90). While Fscn1 belongs to the familiy of actin-binding proteins and organizes F-actin into parallel bundles, it also plays a critical role in cell migration, motility, adhesion and cellular interactions, dihydropyrimidinase-related protein 1 (Crmp1) belongs to the dihydropyrimidinase-likeproteins family which plays an important role in the development and maturation of neurons as well as the axonal growth [52]. The determined upregulation of this protein at the early stage of P7 can be explained by an indication of an increased formation of neuronal components which are required for the synaptic signal transduction for example.

Proteins of the energy metabolism also show a major percentage of differentially regulated proteins within the Cx (total amount of differentially expressed proteins: P7 vs. P90: 9%; P637 vs. P90: 14%). An upregulation of cortical proteins of the energy metabolism was found [53]. With development, the oxidative energy metabolism of the cortex decreases and the adaption to oxidative stress conditions is reduced [54]. Land et al. [55] and Hamada-Kanazawa [56] show that mitochondria increase in the brain by the factor of 6 between P7 and P25. In mitochondria of older animals, a smaller number of respiratory subunits can be found leading to a decrease of energy production [57].

The mitochondria are indirectly involved in the development of neuronal networks and neuronal pasticity (neuronal differentiation, neurite outgrowth, neurotransmitter release as well as the dentritic alteration) by purposing energy components (ATP and NAD$^+$) as well as the regulation of subcellular Ca^{2+} ions and stabilizing the redox-homeostasis [58]. A certain number of proteins of the energy metabolism contribute to these components, subunits of the respiratory chain and the ATP-synthesis. They will be outlined in the following.

Mitochondrial ATP synthase subunit alpha (Atp5a1) is downregulated at developmental stages P7 and P637 compared to P90, whereas the mitochondrial ATP synthase subunit d (Atp5h) shows the same abundance (downregulated at P7 and P637 compared to P90). The protein ATP synthase is a key-protein required for the production of energy. The differential regulation of some of its subunits within the brain region examined indicates an increased abundance of these proteins after P7 (shown in previous paragraph).

The differential regulation of these proteins in the aged rats could be caused by a reaction of the animal to counteract the reduction of the energy production. In addition, several members of the respiratory chain (NADH dehydrogenase [ubiquinone] iron-sulfur protein 2, mitochondrial (Ndufs2), NADH-ubiquinone oxidoreductase 75 kDa subunit, mitochondrial (Ndufs1), NADH dehydrogenase (Ubiquinone) Fe-S protein 3, isoform CRA_c (Ndufs3), NADH dehydrogenase [ubiquinone] flavoprotein 2, mitochondrial (Ndufv2)) are differentially expressed during different stages of development. While Ndufs1, Ndufs2 and Ndufs3 are downregulated at P7 and exhibit no abundance changes around P637 (besides the protein Ndufs1 which is upregulated at P637), Ndufv2 has the identical abundance level at P7 and P90, whereas this protein is found to be absent at P637. In general, the protein NADH dehydrogenase plays an important role in mitochondria. It forms the complex 1 of the respiration chain and links the catalyzation of the oxidation of NADH with the reduction of coenzyme Q. The reduced abundance of NADH dehydrogenase (P7<P90) is probably associated with the ongoing neurogenesis [59], the synaptogenesis and maturation of the neurons coupled with an increased energy consumption [60] after P7 during development. The protein cytochrome b-c1 complex subunit Rieske (Uqcrfs1) shows a downregulation at developmental stage P7 (P7<P90). This protein presents a component of the ubiquinol cytochrome c reductase complex which itself is known to be involved in the production of an electrochemical gradient as well as the resulting synthesis of ATP within the mitochondria. The downregulated subunit of the cytochrome c reductase complex exposes a comparable regulation with the components of the NADH dehydrogenase as was discussed before. The location of these subunits in the mitochondria coincides with similar differential abundances. The differential abundance of this protein may indicate a possible role in the maturation of the Cx especially during neurogenesis.

Regulatory proteins show an obvious differential abundance (total amount of differentially expressed proteins: P7 vs. P90: 13%; P637 vs. P90: 14%). The chaperone like protein DJ-1 (Park7) is downregulated at P7 (P7<P90) and can protect neurons against oxidative stress and cell death. In Western Blot analysis, the downregulation of this protein has been confirmed (Figure 9). As demonstrated by Mitsumoto and Nakagawa [61], DJ-1 may act as an endogenous indicator of oxidative stress and may exhibit an anti-apoptotic effect. As stated by Im et al. [62], Mo et al. [63] and Klawitter et al. [64], this protein also has the ability to inhibit oxidative stress inducing the following apoptosis. Moreover, it has been reported that this protein can prevent apoptotic cell death by recruiting and activating an additional protein (anti-apoptotic protein kinase, Akt) which functions as a serine/threonine-protein kinase and regulates many processes including metabolism, proliferation, cell survival, growth and angiogenesis. A higher abundance of this protein at the adult stage of P90 compared to juvenile rats (P7) could indicate a reaction of the animal to increasing oxidative stress during aging, thus acting as one of the early signs to prevent this factor.

Tropomodulin-2 (Tmod2), the neuronal form of the protein tropomodulin is a regulatory protein downregulated at the stage of P7 (P7<P90). The protein stabilizes the actin filaments and regulates the length of the filaments [65,66]. The regulatory protein cofilin-1 (Cfl1) is also involved in the organization of actin and influences the morphology of cells. The protein is downregulated at P7 in the Cx. In previous studies, an upregulation of this protein could be determined at P7 in other regions of the brain (olfactory bulb, cerebellum) [31,67]. Also Gurniak et al. [68] show that a high abundance of this protein is essential at the early levels of development. For example, the closure of the neural crest combined with the migration of cell populations is

strongly reduced in the absence of this protein. The protein drebrin (Dbn1) shows an upregulation at P7 (P7>P90). This protein is neuron-specific and located in synapses to support neuronal growth. The upregulation of Dbn1 was confirmed in Western Blot analysis at P7 (Figure 9). It was shown that a higher abundance of this protein is present especially between E19 and the first postnatal week. A decreased abundance of Dbn1 seems to be associated with loss of memory in Alzheimer's disease [69].

The protein family of the annexins can bind lipids (mostly acid phospholipids) of the cell membrane with one or several negative charges to oligomerise to trimers or hexamers. If a hexameric formation is established, the requirement for building of transport proteins for ion channels is given. The functional group of the annexins is besides the group of calmodulines necessary for binding calcium [70]. Annexin A6 (Anxa6) shows a downregulation (P7<P90). It is known that the development of the brain and maturation of the rat itself is excessive around P10 and the synaptogenesis sets in during the third and fourth postnatal week [71-73]. Furthermore, Giambanco et al. [74] show that Anxa5 and the accumulation of this protein during the first postnatal week indicates a coincidence of differential regulation and brain development.

The interactions of differential proteins were determined by an induced network module analysis. The consensusPathDB (http://cpdb.molgen.mpg.de/), PANTHER, Reactome and STRING were used to assemble networks of up- and downregulated proteins. The consensusPathDB turned out to generate interactions of differential proteins in one connected component networks. Most of the structural proteins which are differential are downregulated in P7 animals (P7<P90). However, fascin (Fsnc1), drebrin (Dbn1) and Rab GDP dissociation inhibitor beta (Gdi2) are upregulated. Fascin is necessary to form actin bundles of filamentous actin. This is mandatory for mobility and migration. Especially in the early phase of postnatal development these processes seems to be correlated with fascin upregulation found here. Like fascin upregulation is an important factor for neuronal growth. Therefore, drebrin upregulation appears to be associated with the fascin upregulation since both proteins concordantly support processes of neuronal development. In addition, Gdi2 is important for vesicular trafficking that is located within the plasma membrane where neuronal motility as well as neuronal growth are linked. These three upregulated and functionally concurrent proteins have multiple interaction partners in the pathway centric protein analysis found with the consensusPathDB. They can interact on each other upon one intermediate protein, only (Figure 10). It was found that all upregulated P7 proteins can build one connected network component. Hence, these consensual upregulated proteins may interact directly or indirectly to develop structural components of cortical cell populations.

In the P637 group a downregulation of three different ATPases was found: Atp5a1, Atp5h, and Atp6v0d1. After generating the network of protein interactions a massively biochemically interlinked (green dashed lines) subnetwork that is connected with the three differentially expresses ATPases was detected (Figure 11). Downregulation of these 3 ATPases may directly affect such a ATPase-subnetwork in aged rats because most of the other ATPases (magenta names in Figure 11) are direct interaction partners of the downregulated Atp5a1, Atp5h and Atp6v0d1.

In summary, most cytoskeleton proteins (Neurofilaments, β-actin) are downregulated in P7 (P7<P90). Some proteins of migration and motility as well as proteins for maturation and development are upregulated in P7
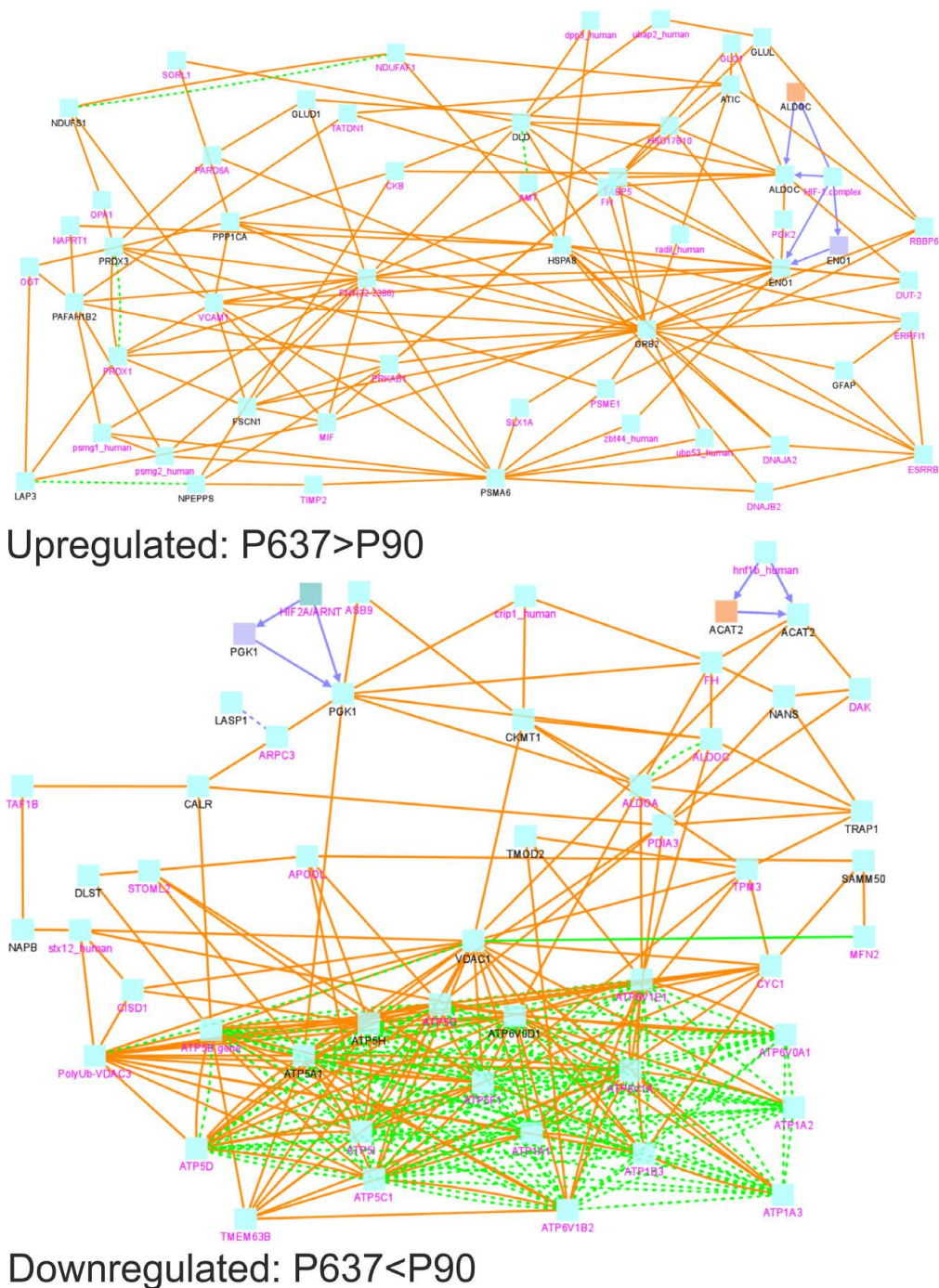
Figure 10: Interactions of upregulated and downregulated proteins of the P7 group. P7 proteins were compared with P90 proteins. Black names: differentially expressed proteins, magenta names: intermediate nodes, orange lines: protein interactions, blue lines: gene regulatory interaction, green lines: biochemical interaction, blue rectangle: gene label, gray rectangle: family unknown.

Figure 11: Interactions of upregulated and downregulated proteins of the P637 group. P637 proteins were compared with P90 proteins. The massive biochemical interactions of different ATPase's are obvious. 3 of them (in black) were downregulated in P637 rats. Black names: differentially expressed proteins, magenta names: intermediate nodes, orange lines: protein interactions, blue lines: gene regulatory interaction, green lines: biochemical interaction, blue rectangle: gene label, orange rectangle: RNA label.

animals (P7>P90). Additionally, Drebrin and Gdi2 which are important for vesicular trafficking and neuronal growth are upregulated in P7 (P7>P90). In aged animals oxidative stress sensors, proteins necessary for autophagy of dysfunctional mitochondria, growth control and hypoxia tolerance (Ppp1ca, Eno1) turned out to be upregulated (P637>P90). Overall, energy consumption and differentiation processes as well as specific regulatory mechanisms can be observed at least indirectly by differential abundances of proteins during ageing.

Acknowledgements

References

1. Cunningham ML, Mac Auley A, Mirkes PE (1994) From gastrulation to neurulation: transition in retinoic acid sensitivity identifies distinct stages of neural patterning in the rat. Dev Dyn 3: 227-241.

2. Adams RJ (1996) Metaphase spindles rotate in the neuroepithelium of rat cerebral cortex. J Neurosci 16: 7610-7618.

3. Adlard BP, Dobbing J, Sands J (1975) A comparison of the effects of cytosine arabinoside and adenine arabinoside on some aspects of brain growth and development in the rat. Br J Pharmacol 54: 33-39.

4. Trojan S, Pokorny J (1999) Theoretical aspects of neuroplasticity. Physiol Res 48: 87-97.

5. Trojan S, Langmeier M, Maresova D, Mourek J, Pokorny J (2004) Plasticity of the brain in neuroontogenesis. Prague Med Rep 105: 97-110.

6. Morris RG, Hebb DO (1999) The Organization of Behavior, Wiley, New York 1949. Brain Res Bull 50: 437.

7. Buonomano DV, Merzenich MM (1998) Cortical plasticity: from synapses to maps. Annu Rev Neurosci 21: 149-186.

8. Bandeira F, Lent R, Herculano-Houzel S (2009) Changing numbers of neuronal and non-neuronal cells underlie postnatal brain growth in the rat. Proc Natl Acad Sci 106: 14108-14113.

9. Kishimoto Y, Davies WE, Radin NS (1965) Developing rat brain: changes in cholesterol, galactolipids, and the individual fatty acids of gangliosides and glycerophosphatides. J Lipid Res 6: 532-536.

10. Cayre M, Canoll P, Goldman JE (2009) Cell migration in the normal and pathological postnatal mammalian brain. Prog Neurobiol 88: 41-63.

11. Bhattacharya B, Saha S, Sarkar PK (1991) Post-transcriptional regulation of tubulin mRNA in developing rat brain. Brain Res Mol Brain Res 10: 347-350.

12. Paxinos G (2004) The Rat Nervous System (3rd edn.). Academic Press; London, UK.

13. Angevine JB, Sidman RL (1961) Autoradiographic study of cell migration during histogenesis of cerebral cortex in the mouse. Nature 192: 766-768.

14. Hicks SP, D'Amato CJ (1968) Cell migrations to the isocortex in the rat. Anat Rec 160: 619-634.

15. Meyer G, Schaaps JP, Moreau L, Goffinet AM (2000) Embryonic and early fetal development of the human neocortex. J Neurosci 20: 1858-1868.

16. Super H, Del Rio JA, Martinez A, Perez-Sust P, Soriano E (2000) Disruption of neuronal migration and radial glia in the developing cerebral cortex following ablation of Cajal-Retzius cells. Cereb Cortex 10: 602-613.

17. Edmondson JC, Hatten ME (1987) Glial-guided granule neuron migration in vitro: a high-resolution time-lapse video microscopic study. J Neurosci 7: 1928-1934.

18. Hatten ME (1990) Riding the glial monorail: a common mechanism for glial-guided neuronal migration in different regions of the developing mammalian brain. Trends Neurosci 13: 179-184.

19. Rakic P (1972) Mode of cell migration to the superficial layers of fetal monkey neocortex. J Comp Neurol 145: 61-83.

20. Kostovic I, Rakic P (1990) Developmental history of the transient subplate zone in the visual and somatosensory cortex of the macaque monkey and human brain. J Comp Neurol 297: 441-470.

21. Shatz CJ, Ghosh A, McConnell SK, Allendoerfer KL, Friauf E, et al. (1990) Pioneer neurons and target selection in cerebral cortical development. Cold Spring Harb Symp Quant Biol 55: 469-480.

22. McConnell SK, Ghosh A, Shatz CJ (1989) Subplate neurons pioneer the first axon pathway from the cerebral cortex. Science 245: 978-982.

23. Doremus TL, Varlinskaya EI, Spear LP (2004) Age-related differences in elevated plus maze behavior between adolescent and adult rats. Ann N Y Acad Sci 1021: 427-430.

24. Hovakimyan M, Haas SJ, Schmitt O, Gerber B, Wree A, et al. (2006) Mesencephalic human neural progenitor cells transplanted into the neonatal hemiparkinsonian rat striatum differentiate into neurons and improve motor behaviour. J Anat 209: 721-732.

25. Haas SJ, Petrov S, Kronenberg G, Schmitt O, Wree A (2008) Orthotopic transplantation of immortalized mesencephalic progenitors (CSM14.1 cells) into the substantia nigra of hemiparkinsonian rats induces neuronal differentiation and motoric improvement. J Anat 212: 19-30.

26. Lessner G, Schmitt O, Haas SJ, Mikkat S, Kreutzer M, et al. (2010) Differential proteome of the striatum from hemiparkinsonian rats displays vivid structural remodeling processes. J Proteome Res 9: 4671-4687.

27. Schwarz SS, Freed WJ (1987) Brain tissue transplantation in neonatal rats prevents a lesion-induced syndrome of adipsia, aphagia and akinesia. Exp Brain Res 65: 449-454.

28. www.criver.com/files/pdfs/rms/rm_rm_r_igs.aspx

29. Pass D, Freeth G (1993) The Rat. Anzccart News 6: 1-4.

30. Klose J, Kobalz U (1995) Two-dimensional electrophoresis of proteins: An updated protocol and implications for a functional analysis of the genome. Electrophoresis 16: 1034-1059.

31. Wille M, Schumann A, Kreutzer M, Glocker MO, Wree A, et al. (2015) The proteome profiles of the olfactory bulb of juvenile, adult and aged rats-an ontogenetic study. Proteome Sci 13: 1-17.

32. Westermeier R (2006) Sensitive, quantitative, and fast modifications for Coomassie Blue staining of polyacrylamide gels. Proteomics 6: 61-64.

33. Lorenz P, Bantscheff M, Ibrahim SM, Thiesen HJ, Glocker MO (2003) Proteome analysis of diseased joints from mice suffering from collagen-induced arthritis. Clin Chem Lab Med 41: 1622-1632.

34. Rower C, Koy C, Hecker M, Reimer T, Gerber B, et al. (2011) Mass spectrometric characterization of protein structure details refines the proteome signature for invasive ductal breast carcinoma. J Am Soc Mass Spectrom 22: 440-456.

35. Konus M, Koy C, Mikkat S, Kreutzer M, Zimmermann R, et al. (2013) Molecular adaptations of Helicoverpa armigera midgut tissue under pyrethroid insecticide stress characterized by differential proteome analysis and enzyme activity assays. Genom Proteom 8: 152-162.

36. Becker M, Schindler J, Nothwang HG (2006) Neuroproteomics-the tasks lying ahead. Electrophoresis 27: 2819-2829.

37. Schneider LV, Hall MP (2005) Stable isotope methods for high-precision proteomics. Drug Discov Today 10: 353-363.

38. Takei N, Kondo J, Nagaike K, Ohsawa K, Kato K, et al. (1991) Neuronal survivalfactor from bovine brain is identical to neuron-specific enolase. J Neurochem 57: 1178-1184.

39. Wilbur DO, Patel MS (1974) Development of mitochondrial pyruvate metabolism in rat brain. J Neurochem 22: 709-715.

40. Lockwood A, Bailey E (1971) The course of ketosis and the activity of key enzymes of ketogenesis and ketone-body utilization during development of the postnatal rat. Biochem J 124: 249-254.

41. Vannucci RC, Vannucci SJ (2000) Glucose metabolism in the developing brain. Semin Perinatol 24: 107-115.

42. Vannucci RC, Christensen MA, Stein DT (1989) Regional cerebral glucose utilization in the immature rat: Effect of hypoxia-ischemia. Pediatr Res 26: 208-214.

43. Devaux S, Poulain FE, Devignot V, Lachkar S, Irinopoulou T, et al. (2012) Specific serine-proline phosphorylation and glycogen synthase kinase 3β-directed subcellular targeting of stathmin 3/Sclip in neurons. J Biol Chem 287: 22341-22353.

44. Kinoshita A, Noda M, Kinoshita M (2000) Differential localization of septins in the mouse brain. J Comp Neurol 428: 223-239.

45. Xue J, Tsang CW, Gai WP, Malladi CS, Trimble WS, et al. (2004) Septin 3 (G-septin) is a developmentally regulated phosphoprotein enriched in presynaptic nerve terminals. J Neurochem 91: 579-590.

46. Takamori S, Holt M, Stenius K, Lemke EA, Grønborg M, et al. (2006) Molecular anatomy of a trafficking organelle. Cell 127: 831-846.

47. Pernier J, Shekhar S, Jegou A, Guichard B, Carlier MF (2016) Profilin interaction with actin filament barbed end controls dynamic instability, capping, branching, and motility. Dev Cell 36: 201-214.

48. Mostowy S, Cossart P (2012) Septins: the fourth component of the cytoskeleton. Nat Rev Mol Cell Biol 13: 183-194.

49. Cho SJ, Lee H, Dutta S, Song J, Walikonis R, et al. (2011) Septin 6 regulates the cytoarchitecture of neurons through localization at dendritic branch points and bases of protrusions. Mol Cells 32: 89-98.

50. Maurya DK, Sundaram CS, Bhargava P (2009) Proteome profile of the mature rat olfactory bulb. Proteomics 9: 2593-2599.

51. Riederer BM, Porchet R, Marugg RA (1996) Differential expression and modification of neurofilament triplet proteins during cat cerebellar development. J Comp Neurol 364: 704-717.

52. Yoshimura T, Kawano Y, Arimura N, Kawabata S, Kikuchi A, et al. (2005) GSK-3 beta regulates phosphorylation of CRMP-2 and neuronal polarity. Cell 120: 137-149.

53. Yan LJ, Thangthaeng N, Forster MJ (2008) Changes in dihydrolipoamide dehydrogenase expression and activity during postnatal development and aging in the rat brain. Mech Ageing Dev 129: 282-290.

54. Villa RF, Gorini A, Ferrari F, Hoyer S (2013) Energy metabolism of cerebral mitochondria during aging, ischemia and post-ischemic recovery assessed by functional proteomics of enzymes. Neurochem Int 63: 765-781.

55. Land JM, Booth RF, Berger R, Clark JB (1977) Development of mitochondrial energy metabolism in rat brain. Biochem J 164: 339-448.

56. Hamada-Kanazawa M, Narahara M, Takano M, Min KS, Tanaka K, et al. (2011) β-Citryl-L-glutamate acts as an iron carrier to activate aconitase activity. Biol Pharm Bull 34: 1455-1464.

57. Turpeenoja L, Villa RF, Magri G, Giuffrida Stella AM (1988) Changes of mitochondrial membrane proteins in rat cerebellum during aging. Neurochem Res 13: 859-865.

58. Cheng A, Hou Y, Mattson MP (2010) Mitochondria and neuroplasticity. ASN Neuro 2: e00045.

59. Finlay BL, Darlington RB (1995) Linked regularities in the development and evolution of mammalian brains. Science 268: 1578-1584.

60. Attwell D, Laughlin SB (2001) An energy budget for signaling in the grey matter of the brain. J Cereb Blood Flow Metab 21: 1133-1145.

61. Mitsumoto A, Nakagawa Y (2001) DJ-1 is an indicator for endogenous reactive oxygen species elicited by endotoxin. Free Radic Res 35: 885-893.

62. Im JY, Lee KW, Junn E, Mouradian MM (2010) DJ-1 protects against oxidative damage by regulating the thioredoxin/ASK1 complex. Neurosci Res 67: 203-208.

63. Mo JS, Jung J, Yoon JH, Hong JA, Kim MY, et al. (2010) DJ-1 modulates the p38 mitogen-activated protein kinase pathway through physical interaction with apoptosis signal-regulating kinase 1. J Cell Biochem 110: 229-237.

64. Klawitter J, Agardi E, Corby K, Leibfritz D, Lowes BD, et al. (2013) Association of DJ-1/PTEN/AKT- and ASK1/p38-mediated cell signalling with ischaemic cardiomyopathy. Cardiovasc Res 97: 66-76.

65. Kong J, Xu Z (1998) Massive mitochondrial degeneration in motor neurons triggers the onset of amyotrophic lateral sclerosis in mice expressing a mutant SOD1. J Neurosci 18: 3241-3250.

66. Kostyukova AS, Rapp BA, Choy A, Greenfield NJ, Hitchcock-De Gregori SE (2005) Structural requirements of tropomodulin for tropomyosin binding and actin filament capping. Biochemistry 44: 4905-4910.

67. Wille M, Schümann A, Wree A, Kreutzer M, Glocker MO, et al. (2015) The Proteome Profiles of the Cerebellum of Juvenile, Adult and Aged Rats--An Ontogenetic Study. Int J Mol Sc 16: 21454-21485.

68. Gurniak CB, Perlas E, Witke W (2005) The actin depolymerizing factor n-cofilin is essential for neural tube morphogenesis and neural crest cell migration. Dev Biol 278: 231-241.

69. Gerdin AK (2010) The Sanger Mouse Genetics Programme: high throughput characterisation of knockout mice. Acta Ophthalmologica 88: 925-927.

70. McNeil AK, Rescher U, Gerke V, McNeil PL (2006) Requirement for annexin A1 in plasma membrane repair. J Biol Chem 46: 35202-35207.

71. Eayrs JT, Goodhead B (1959) Postnatal development of the cerebral cortex in the rat. J Anat 93: 385-402.

72. Aghajanian GK, Bloom FE (1967) The formation of synaptic junctions in developing rat brain: a quantitative electron microscopic study. Brain Res 6: 716-727.

73. Caley DW, Maxwell DS (1968) An electron microscopic study of neurons during postnatal development of the rat cerebral cortex. J Comp Neurol 133: 17-44.

74. Giambanco I, Verzini M, Donato R (1993) Annexins V and VI in rat tissues during postnatal development: immunochemical measurements. Biochem Biophys Res Commun 196: 1221-1226.